LAWRENCE
LIVERMORE
NATIONAL
LABORATORY

UCRL-JRNL-205365

Crystallography of the Delta to Alpha Martensitic Transformation in Plutonium Alloys

Y.M. Jin, Y.U. Wang, A.G. Khachaturyan, C.R. Krenn, A.J. Schwartz

July 21, 2004

Metallurgical Transactions A

Crystallography of the $\delta \rightarrow \alpha$ Martensitic Transformation in Plutonium Alloys

Y. M. Jin, Y. U. Wang, A. G. Khachaturyan*
Department of Ceramic and Materials Engineering, Rutgers University,
607 Taylor Road, Piscataway, NJ 08854

C. R. Krenn, A. J. Schwartz
Chemistry and Materials Science Directorate, Lawrence Livermore National Laboratory,
University of California, Livermore, California 94551

Abstract

A new stress-accommodating crystallographic mechanism of the $\delta \rightarrow \alpha$ martensitic transformation in plutonium alloys is proposed. According to this mechanism, an orientation variant of the α phase is produced by a combination of a homogeneous strain and shuffling of the alternating close-packed $(111)_\delta$ planes. It is shown that the formation of stable transformation-induced twins whose twin plane orientations and twin shear directions do not depend on the small variations of the crystal lattice parameters is the preferred stress-accommodating mode. Only these stable twins have dislocation-free twin boundaries while the twin boundaries of all others are decorated by ultra-dense distribution of partial dislocations. The theory predicts a crystal lattice rearrangement mechanism involving the $(205)_\alpha$ ($(01\bar{1})_\delta$) stable twins. The corresponding Invariant Plane Strain solutions, with special emphasis on two simplest shuffling modes, the single and double elementary modes, are presented and compared with the existing experimental observations. It is shown that the habit plane orientation is highly sensitive to the input values of the crystal lattice parameters and especially to the accuracy of the measured volume change in the $\delta \rightarrow \alpha$ transformation. An analysis of these effects on the habit plane orientation and orientation relations is also presented.

1. Introduction

Research on plutonium metal and its alloys has been carried out due to its extreme importance as a reactive nuclear metal and because of its unique physical properties. Plutonium transforms between six distinct crystallographic phases (the most of any element) when heated to its melting point from room temperature under atmospheric pressure. The low-symmetry monoclinic α phase is stable at room temperature, but it is a brittle material difficult for machining. The high temperature δ phase has the face-centered cubic (FCC) structure, which is ductile enough to be machined and can be stabilized down to relatively low temperatures by alloying it with a small amount of gallium. However, δ phase is not stable under pressure or at cryogenic temperatures — it

* To whom correspondences should be addressed.

transforms to the α phase with a volume change (contraction) as much as 20% (the largest such change known). The reversal of this transformation occurs under hydrostatic tension or heating. The study of the phase transformation between δ and α phases is an important topic both technically and scientifically. Although it is common practice to distinquish between the equilibrium α phase with a low gallium content and a metastable α′ phase formed martensitically that has a supersaturation of gallium [1], in this paper, we refer to both forms as α. A comprehensive review on the physical properties of plutonium and relevant research works can be found in [1].

The δ→α transformation is a martensitic (displacive) transformation [2]. The unusually large volume change distinguishes it from other martensitic transformations (MTs) and makes it an interesting topic from both scientific and engineering viewpoints. A starting point of any study of MTs is establishing the Bain distortion, i.e., the crystal lattice rearrangement that transforms the homogeneous parent lattice into the homogeneous lattice of the martensitic phase. Finding the Bain distortion requires a determination of the crystal lattice correspondence between the crystal lattices of the parent and martensitic phases. So far, this correspondence has not been clearly defined experimentally due to the complicated α phase crystallography and limited experiments.

The theoretical investigation of this system plays an especially important role because of the difficulties in its experimental study. There are several aspects of the MT in plutonium that have to be addressed. They are the morphology of the martensitic phase, the transformation hysteresis, and the response to applied stress. In particular, these aspects could be investigated via 3D computational modeling (such as that in [3]). However, to carry out such modeling, we have to know the crystallographic mechanism of the δ→α crystal lattice rearrangement. The experimental observations and the theoretical works on the crystallographic features of α phase and the δ→α transformation are reported in [2, 4-18]. Several possible lattice correspondences relating the FCC δ phase to the monoclinic α phase were first proposed by Olson and Adler [2], and the possible twin modes and slip accommodation modes have been studied by various researchers [2, 4, 6-8, 10]. However, given the facts that previous studies investigated a limited number of possible δ→α crystal lattice rearrangements and that the existing theoretical models are insufficient to explain existing experimental observations [8-18], the crystallographic mechanism of this transformation is still open for further investigation.

In this study, we employ the crystallographic theory of MTs [19, 20], which is an advanced version of the traditional geometric theory [21, 22]. We consider all possible δ→α crystal lattice rearrangements consistent with the crystal lattice parameters of the phases and shuffling of close packed planes. The theoretical analysis provides a selection of optimal crystal lattice rearrangements, transformation twins, orientation relations, and habit plane orientations of the α phase crystals based on strain energy minimization and stable transformation twin formation criteria.

1.1. Elastic Energy Accompanying Martensitic Transformation

The MT proceeds by diffusionless (displacive) formation of martensitic phase "islands" within a parent phase crystal lattice. These islands are different orientation domains (variants) of the martensitic phase. Since the transformation results in a crystal lattice misfit between the martensitic domains of different orientations and between the martensitic domains and parent phase, it generates elastic strain. The elastic strain energy of formation of the isolated domains is usually too large to allow the transformation to proceed. It is proportional to the volume, *V*, of the martensitic phase and is of the order of

$$E_{\text{volume}} \sim \mu_t \varepsilon_0^2 V \,, \tag{1}$$

where μ_t is the typical elastic modulus and ε_0 is the stress-free transformation strain. However, this volume-dependent elastic energy can be eliminated if the domains aggregate to form a special stress-accommodating domain structure. This structure should meet certain conditions as are discussed in the following.

The stress generated by the crystal lattice misfit between the martensitic domains with different orientations is completely eliminated if the crystal lattices of these domains perfectly fit along their interfaces and thus do not generate interfacial strain energy. This optimal configuration is achieved if the domain structure is a multilayer consisting of alternating twin-related lamellae of different orientation domains and the interfaces are parallel to the twin plane, as shown in Fig. 1. Geometrically, this structure is the same as the polytwinned structure with regularly repeated twin boundaries.

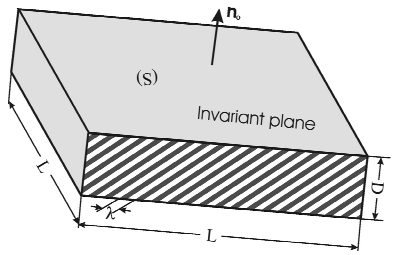

Figure 1. Schematic of polytwinned plate consisting of alternating lamellae of two twin-related martensitic variants.

The macroscopic shape change of this multilayer aggregate in the unconstrained (stress-free) state is determined by the domain-averaged transformation strain over the aggregate. Since the aggregate is imbedded into the parent phase matrix, its shape change caused by the transformation generates elastic strain and thus results in a raise of the volume-dependent strain energy (1). However, this part of the strain energy can be mostly eliminated as well if the relation between the thicknesses of the twin-related domain layers in the aggregate is such that the domain-averaged transformation strain is an Invariant Plane Strain (IPS) and the multilayer aggregate is a plate whose habit plane is an invariant plane that is not affected by the transformation [19, 23, 24]. To be an IPS, the domain-averaged transformation matrix has to be

$$< \hat{\mathbf{A}} >_{ij} = \delta_{ij} + \varepsilon \, l_i n_j \,, \tag{2a}$$

where δ_{ij} is the Kronecker delta (i.e., $\delta_{ij} = 1$ if $i = j$ and $\delta_{ij} = 0$ if $i \neq j$), ε is the magnitude of the strain describing the macroscopic shape change, $\mathbf{l}$ is a unit vector in the direction of the displacement produced by the IPS, and $\mathbf{n}$ is the unit vector normal to the invariant plane. In this case, the habit plane interface between the martensite and parent phase

normal to **n** is macroscopically invariant, i.e., it does not generate martensite/parent phase misfit at the macroscopic scale, which is a scale greater than the typical thickness of lamellar domains, λ. Therefore, the domain-averaged IPS eliminates the long-range elastic strain at distances exceeding the domain thickness, λ, and results in the vanishing of the volume-dependent strain energy (1). The internal structure of the plate consisting of alternating twin-related lamellar martensitic domains parallel to the twin plane is illustrated in Fig. 1.

Without a loss of generality, the IPS transformation matrix (2a) can always be written as:

$$< \hat{\mathbf{A}} >_{ij} = \delta_{ij} + \varepsilon_{\mathrm{s}}\, s_i n_j + \varepsilon_{\mathrm{n}}\, n_i n_j\,, \tag{2b}$$

where ε_{s} is the shear component of the shape strain ε, ε_{n} is the normal component, and **s** is a unit vector in the shear direction. The strain component ε_{n} characterizes the volume change and is a material constant dependent on the crystal lattice parameters of the parent and martensitic phases rather than on the transformation mechanism.

The domain structure with the domain-averaged IPS shown in Fig. 1 eliminates only the volume-dependent strain energy associated with the long-range strain. The remaining part of the strain energy is proportional to the habit plane surface area, *S*, and is associated with the short-range strain localized within a layer adjacent to the plate surface, the thickness of the layer being of the same order as the typical thickness of the domains, λ, [19]:

$$E_{\mathrm{surface}} = \xi_1 \mu_{\mathrm{t}} \varepsilon_{\mathrm{twin}}^2 \lambda\, S\,, \tag{3a}$$

where $\varepsilon_{\mathrm{twin}}$ is the twin strain that transforms the crystal lattice of an orientation domain into the crystal lattice of its twin-related adjacent domain, and ξ_1 is a dimensionless coefficient. Since the $\delta \rightarrow \alpha$ transformation of plutonium involves shuffling (see Section 2), partial dislocations are piled up at the domain boundaries, which modifies Eq. (3a) to:

$$E_{\mathrm{surface}} = \xi_1 \mu_{\mathrm{t}} \varepsilon_{\mathrm{twin}}^2 \lambda\, S + \xi_2 \gamma S\,, \tag{3b}$$

where ξ_2 is a dimensionless coefficient, and γ is the interface energy associated with the partial dislocation distribution on the domain boundaries that is a result of the specific shuffling mode involved. It should be noted that ξ_1 and ξ_2 depend on the geometry of habit plane and twins. Finding these coefficients requires the explicit solution of the elasticity equation.

Finally, there is a remnant of the strain energy generated by the crystal lattice misfit along the interfacial boundary at the edge of the martensite plate. The corresponding strain energy depends on the thickness of the plate, *D*, and its perimeter, *P*:

$$E_{\mathrm{edge}} = \xi_3 \mu_{\mathrm{t}} \varepsilon^2 D^2 P\,, \tag{4}$$

where ξ_3 is again a dimensionless coefficient, whose value is determined by the explicit solution of the elasticity equation. This strain energy proportional to the martensite plate perimeter, in fact, has the same form as that of a dislocation loop in the habit plane

normal to **n** with a Burgers vector $b = \varepsilon D$, where ε is the shape strain in Eq. (2a) determined by domain-averaging [19].

As mentioned above, the lattice correspondences between the δ and α plutonium phases are not conclusively known; neither is the crystal lattice rearrangement producing a homogeneous single domain of the α phase in the δ→α transformation. The strain produced by such a rearrangement is called a Bain distortion, and it has to be determined first in order to proceed to the determination of the crystallographic mechanism of the transformation and the habit plane orientation. It is assumed that one criterion for a choice of the Bain distortion is a strain energy minimization. It is reduced to the minimization of the three contributions of the strain energy given by Eqs. (1), (3b) and (4).

The volume-dependent contribution to the strain energy (1) vanishes if the domain-averaged stress-free transformation strain is an IPS. A minimization of the surface-dependent part of the strain energy (3b) is another criterion for a choice of the Bain distortion and determines a choice of the twin-related orientation domain pair comprising a martensite plate. The exact energy minimization condition requires the explicit solution of (3b). As will be shown, the requirement of a stable transformation twin plays a key role in selecting twin pairs as well as the Bain distortion for the plutonium MT.

Finally, a minimization of the edge-dependent part of the strain energy (4) is reduced to finding the Bain distortion and the selection of twin-related domain pairs that provide the minimum value of the domain-averaged shape strain ε. As discussed above with respect to Eq. (2b), the strain component ε_n does not depend on a choice of the δ→α transformation mechanism. Therefore, the minimization of the strain energy (4) is equivalent to finding the types of domains providing the minimum value of the shear strain component ε_s.

The MT does not occur if the first criterion is not met because the positive volume-dependent contribution dominates the strain energy opposing the transformation. The second criterion is related to a minimization of the surface-dependent strain energy contribution and is less critical. The third criterion plays a minor role since the edge-dependent elastic energy is proportional to the plate perimeter and thus provides the smallest contribution to the strain energy. The second and third criteria should be considered only when the first criterion is met.

In this paper we will focus on the IPS condition in the elastic energy minimization in order to eliminate the main contribution to elastic energy. The surface-dependent strain energy is considered secondarily. As will be shown, the IPS condition together with the stable transformation twin condition drastically narrows the scope of possible crystal lattice rearrangement mechanisms to limited numbers that can be further selected by taking into account the existing experimental observations.

To satisfy the first criterion, i.e., eliminating the volume-dependent strain energy (1) by IPS, we employ the crystallographic analysis proposed by Khachaturyan [19] and

further developed by Jin and Weng [20]. This analysis considers the domain-averaged transformation strains produced by all possible twin-related orientation domain pairs comprising a martensite plate.

If we know a single Bain distortion, say $\hat{\mathbf{B}}(1)$, the rotation and reflection symmetry elements of the FCC δ phase generate the other 23 Bain distortion matrices, $\hat{\mathbf{B}}(2)$, …, $\hat{\mathbf{B}}(24)$, which are 24 crystallographically equivalent orientation domains of the monoclinic α phase. Therefore, there are 276 (24×23÷2) possible twin-related domain pairs (only some of which can really form transformation twins). Fortunately, we do not have to consider all of them. It is sufficient to consider only 23 different pairs formed by any orientation domain (i.e. variant 1) with each of the remaining 23 orientation domains and, thus, we need to carry out a comparative analysis of the 23 domain pairs — all other pairs are crystallographically equivalent to the considered ones and differ by just a symmetry operation of the FCC δ phase. The comparative analysis should consist of two steps corresponding to the IPS criterion mentioned above and the stable twin condition. The first step is a test whether the individual domain pairs are able to form twins and provide the domain-averaged IPS. The domain pairs passing this test are further tested against the criteria of a successful formation of a stable twin.

A task of analyzing the 23 domain pairs, i.e., finding the twins that provide IPS, is still complicated due to the fact that the choice of the Bain matrix is not unique. The latter further increases the number of possible candidates for the optimal Bain distortion pairs. This is a formidable task that can be done only by an appropriate computer program. Such an analysis is presented in this paper.

1.2. Invariant Plane Strain Transformation

For a given pair of domains produced, for example, by the Bain distortions $\hat{\mathbf{B}}(1)$ and $\hat{\mathbf{B}}(2)$, we first examine if this domain pair can form a transformation twin [20]. It should be mentioned here that the transformation twin and deformation twin have different natures although they are the same geometrical object. A transformation twin is formed from a bi-layer of domains of martensite variants (twin-related domains), the interface being a boundary between different variants. A deformation twin is the result of mechanical twinning during plastic deformation. The twins considered in this paper are transformation-induced twins. If a given pair of domains can form a misfit-free multilayer, this domain pair is a set of twin-related variants. For a martensite plate consisting of twin-related orientation variants 1 and 2, we present the domain-averaged transformation matrix as [19, 20]:

$$< \hat{\mathbf{A}} >= \hat{\mathbf{R}}_{\text{plate}} \, [x\hat{\mathbf{B}}(1) + (1-x)\hat{\mathbf{R}}_{\text{twin}}\hat{\mathbf{B}}(2)], \tag{5}$$

where $\hat{\mathbf{R}}_{\text{plate}}$ is the rotation of the polytwinned plate required for a continuity of the lattice at the boundary between the plate and the matrix, $\hat{\mathbf{R}}_{\text{twin}}$ is the rotation of the second orientation domain required for a continuity of the lattice across the twin plane, and x is the volume fraction of the first orientation domain.

To provide an IPS, the volume fraction x has to be chosen so that the domain-averaged transformation matrix has a dyadic form given by Eq. (2a). Then the habit plane of the polydomain plate is normal to **n**. The vector $\varepsilon\,\mathbf{l}$ describes the macroscopic shape change produced by a formation of the martensite plate. By definition, the volume fraction x of the domains meets the condition $0 < x < 1$. If x providing the IPS is 1 or 0, this means that the single domain martensite plate has an invariant plane habit and thus eliminates the volume-dependent elastic energy (1). Such a scenario is practically never observed. If Eq. (5) is not reduced to Eq. (2) at any x, the orientation domains of the chosen pair do not meet the first criterion (IPS condition) and thus should be rejected.

In general, not all of the 23 domain pairs that have been tested can form transformation twins, and only a few of the twin-related pairs may be able to provide IPS. Among the domain pairs satisfying the first criterion, we determine the optimal Bain distortion matrices produced by a twin-related pair, say again, $\hat{\mathbf{B}}(1)$ and $\hat{\mathbf{B}}(2)$ that provide IPS. This optimal Bain distortion should provide a stable twin (the stability of transformation twins will be discussed in the next section). Once the optimal Bain distortion matrix is found, we can predict the type of twin-related domains that produce transformation twins. The determination of the volume fraction x predicts the habit plane orientation. Finally, the matrix $\hat{\mathbf{R}}_{\text{plate}}\hat{\mathbf{B}}(1)$ or $\hat{\mathbf{R}}_{\text{plate}}\hat{\mathbf{R}}_{\text{twin}}\hat{\mathbf{B}}(2)$ determines the orientation relations between martensite and parent phase.

1.3. Stable Transformation Twin

We first briefly explain the notations used to describe twins. A twin is conventionally described by its twin elements: directional vector pairs, K and η, and scalar s. The element K is a designation of the twin plane normal, η the direction of shear, and s the magnitude of twin shear (i.e., twin strain $\varepsilon_{\text{twin}}$ in Eq. (3)). For a given crystal lattice that forms twins, there are always two twin solutions [20]: (K_1, η_1, s) and (K_2,η_2, s), both of which can serve as a twin. We call the twin along η_2 direction on K_2 plane a conjugate of the twin along η_1 direction on K_1 plane, and vice versa.

Let us consider the Bain distortion matrices of one pair of twin-related martensite variants, e.g. $\hat{\mathbf{B}}(1)$ and $\hat{\mathbf{B}}(2)$. They are continuous functions of the lattice parameters of parent and product phase: a_0, a, b, c, β. All these parameters are intrinsic parameters, which do not depend on the crystal structure rearrangement mechanism. The twins can be grouped into two kinds: (1) those whose twin plane and twin shear direction (K,η) depend on the specific values of crystal lattice parameters of the parent and product phases and change when the latter changes; and (2) those for which K and η depend only on the crystallographic symmetry of the parent and product phases and do not change under small variations of the lattice parameters. The first kind of twin would result in a continuous gradual change in the twin plane orientation with the temperature, composition, and other external thermodynamic parameters affecting crystal lattice parameters. This is a phenomenon that has never been observed. We will call these twins

of unstable geometry *unstable twins*. The second kind of twins has stable geometry that is not affected by gradual change of the crystal lattice parameters and thus by the change of the temperature and composition. We call these twins *stable twins*. Since the stable twins are the only ones that have been observed, we analyze below only those crystal lattice rearrangement mechanisms that produce stable twins. This requirement of stable twin formation serves as the second criterion to select the Bain distortion.

2. Lattice Correspondence and Bain Distortion

Unlike the traditional cases of the MT in Fe-base alloys where the Bain distortion is characterized by a homogeneous strain, the Bain distortion in plutonium is a combination of a homogeneous distortion and a shuffling. The FCC δ phase lattice is a three-layer structure formed by the ...*ABCABC*... stacking of the close-packed $(111)_\delta$ atomic layers, while the monoclinic α phase lattice is a two-layer structure formed by the ...$A'B'A'B'A'B'$... sequence of the quasi-close-packed $(010)_\alpha$ atomic layers. The latter structure is formed by the $\delta\rightarrow\alpha$ crystal lattice rearrangement of the FCC δ phase. This rearrangement can be divided into three steps. The first step is a shuffling that leads to the formation of a two-layer hexagonal close-packed (HCP) structure ...*ABABAB*... from the three-layer FCC structure ...*ABCABC*... of the δ phase lattice. The FCC→HCP transition occurs by rigid body translations of alternating $(111)_\delta$ atomic layers along any of the three partial δ lattice translation vectors: $1/6[\,\bar{2}\,1\,1\,]_\delta$, $1/6[\,1\,\bar{2}\,1\,]_\delta$ or $1/6[\,1\,1\,\bar{2}\,]_\delta$. This HCP lattice is a transient structure during the $\delta\rightarrow\alpha$ transformation.

The shuffling resulting in the FCC→HCP transition is not unique. There are many ways of $(111)_\delta$ plane shuffling that produce the same transient HCP lattice. These shufflings could be any operations of three crystallographically equivalent partial translations. In particular, applications of m_1 times $1/6[\,\bar{2}\,1\,1\,]_\delta$, m_2 times $1/6[\,1\,\bar{2}\,1\,]_\delta$ and m_3 times $1/6[\,1\,1\,\bar{2}\,]_\delta$ to alternating FCC ...*ABCABC*... stacking planes produce the same transient HCP ...*ABABAB*... structure. However, each shuffling producing the same HCP lattice gives a net average displacement $\bar{\mathbf{h}}$ which depends on $(m_1\ m_2\ m_3)$, as calculated for each two close-packed layers (period) of the transient HCP lattice:

$$\bar{\mathbf{h}} = \frac{1}{m_1+m_2+m_3}\left[\frac{m_1}{6}[\,\bar{2}\,1\,1\,]_\delta + \frac{m_2}{6}[\,1\,\bar{2}\,1\,]_\delta + \frac{m_3}{6}[\,1\,1\,\bar{2}\,]_\delta\right]. \qquad (6)$$

The set of integers $(m_1\ m_2\ m_3)$ gives the period of shuffling as $2(m_1+m_2+m_3)$ close-packed layers. It follows from Eq. (6) that all possible vectors $\bar{\mathbf{h}}$ are mapped onto the area covered by the triangle ABC drawn in the close-packed plane and shown in Fig.2. The center of this triangle (point "O") coincides with an FCC lattice site. In Fig. 2, an $\bar{\mathbf{h}}$ vector starts at point "O" and ends at a point either in the interior or on the sides of the triangle. Any vertex of this triangle corresponds to a situation where shuffling occurs by a set of partial lattice translations in the $(111)_\delta$ plane along one of the $<11\bar{2}>_\delta$ directions. A point on the sides of this triangle corresponds to shuffling by a set of partial

translations along two of the $<11\bar{2}>_\delta$ directions. A point inside this triangle corresponds to shuffling involving partial translations along all three $<11\bar{2}>_\delta$ directions.

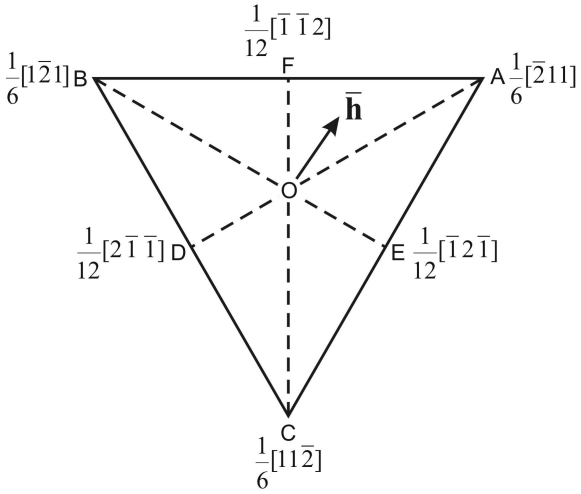

Figure 2. All possible average displacement vectors $\bar{\mathbf{h}}$ are mapped onto the area of the triangle ABC drawn in the closed-packed plane with its center "O" coinciding with a FCC lattice site. An $\bar{\mathbf{h}}$ vector starts at point "O" and ends at a point within this area. The dashed lines indicate special $\bar{\mathbf{h}}$ vectors that provide stable transformation twins.

The displacement vector $\bar{\mathbf{h}}$ results in the crystal lattice rearrangement $\hat{\mathbf{A}}(1)$ corresponding to the macroscopic shear transformation matrix:

$$\hat{\mathbf{A}}(1)_{ij} = \delta_{ij} + \frac{\sqrt{3}}{2}\bar{h}_i\, v_j^{[111]_\delta}, \tag{7}$$

where $\mathbf{v}^{[111]_\delta}$ is unit vector along $[111]_\delta$. The lattice correspondence in the normal direction of the basal plane is

$$\frac{2}{3}[\,1\,1\,1\,]_\delta - \bar{\mathbf{h}} \rightarrow [\,0\,1\,0\,]_\alpha . \tag{8}$$

To produce the crystal lattice of the monoclinic α phase from this transient HCP lattice, we have to make second and third steps. The second step is a homogeneous transformation of the transient HCP structure, and the third step completing the δ→α transformation is a set of periodic (and commensurate) displacements of the plutonium atoms from the sites of the transformed HCP structure. By definition, the periodic displacements, unlike the shuffling of the $(111)_\delta$ planes in the first step or the homogeneous strain in the second step, do not change the macroscopic shape of the transformed volume and thus are not relevant to an elastic energy analysis. However, they determine a choice of the unit cell that is the periodically repeated motif of the α phase lattice. The periods of the displacements are the elementary translations determining a unit cell of the α phase. Since a unit cell of the α phase has 16 plutonium atoms with 8 atoms in each *A*' and *B*' layers, the unit cell of the transient HCP lattice, which is transformed into the unit cell of the α phase lattice in this third step, should also

be enlarged to include 8 atoms in each layer. To maintain the two-layer structure, the enlargement of the unit cell is along the *A* and *B* layers of the HCP lattice. This mechanism provides the $(111)_\delta \,||\, (010)_\alpha$ orientation relation.

An enlarged unit cell in each layer of the transient HCP lattice meeting these requirements is not unambiguous. However, the best choice for the enlarged unit cell in the HCP lattice is the one that involves the smallest homogeneous strain transforming a unit cell of the transient HCP lattice to that of the α phase. This is because the smallest homogeneous strain generates the lowest elastic energy. Examples of different choices of unit cells with 8 atoms per close-packed plane, which may transform to the unit cell of the α phase by appropriate homogeneous strain, are shown in Fig. 3. The α phase unit cell is also shown in Fig. 3. In Fig. 3 the following crystallographic data [10] are used:

δ phase: $a_0 = 0.46256nm$,

α phase: $a = 0.61991nm$, $b = 0.48367nm$, $c = 1.09637nm$, $\beta = 101.79^o$. (9)

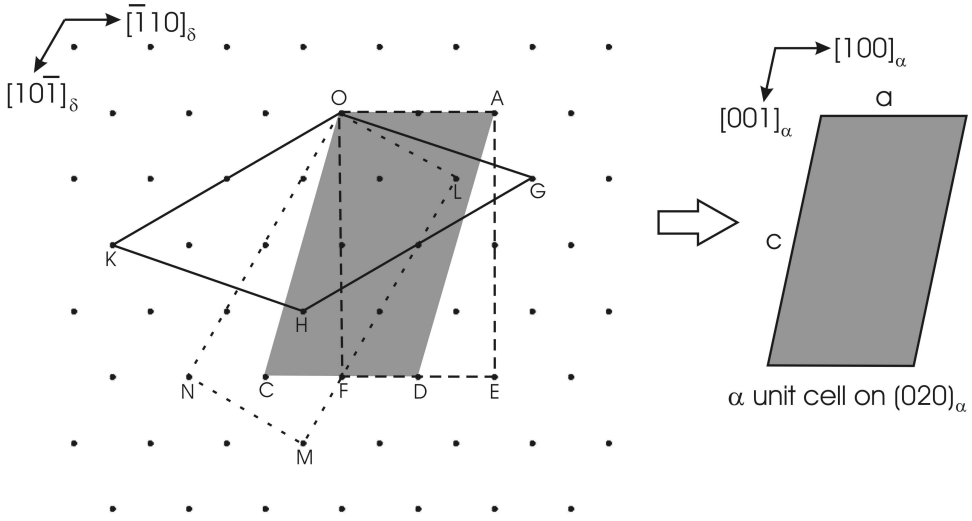

Figure 3. *Left*: The lattice in the close-packed $(111)_\delta$ plane of the FCC δ phase, which is the same as the closed-packed plane of the transient HCP structure prior to the homogeneous transformation. OADC, OAEF, OGHK, and OLMN are examples of choices of unit cells with 8 atoms per unit cell of each close-packed plane, which can form the unit cell of the α phase in its (010) plane. *Right*: An α phase unit cell in the $(010)_\alpha$ plane. The basal plane transformation is characterized by the homogeneous strain of a unit cell including 8 atoms in the $(111)_\delta$ plane to the α phase unit cell. OADC is the cell requiring the least basal plane strain and which minimizes the elastic energy of transformation.

The OADC unit cell is the best choice because it requires the minimum strain of the basal plane. In the unit cell OADC, $\mathrm{OA} = [\bar{1}10]_\delta$ and $\mathrm{OC} = 1/2\,[31\bar{4}]_\delta$, and this results in the lattice correspondences:

$$[\,\bar{1}10\,]_\delta \rightarrow [\,100\,]_\alpha,\ \frac{1}{2}[\,31\bar{4}\,]_\delta \rightarrow [\,001\,]_\alpha. \qquad (10)$$

The lattice correspondences (8) and (10) were first proposed in [2] and have been used in all later crystallographic works [6, 7, 10]. Using relations (10), the above mentioned three partial δ lattice translation vectors, $1/6[\,\bar{2}\,1\,1\,]_\delta$, $1/6[\,1\,\bar{2}\,1\,]_\delta$ and $1/6[\,1\,1\,\bar{2}\,]_\delta$, correspond to the partial α lattice translation vectors, $1/24[\,\bar{5}\,0\,2\,]_\alpha$, $1/24[\,\bar{7}\,0\,\bar{2}\,]_\alpha$ and $1/12[\,1\,0\,2\,]_\alpha$, respectively. The *b* axis of the monoclinic α phase is perpendicular to the close-packed plane and stays parallel to the hexagonal axis of the transient HCP structure, i.e., the *b* axis of the α phase is perpendicular to the $(111)_\delta$ plane.

The homogeneous transformation matrix from the *A* and *B* layers of the transient HCP lattice to the *A*' and *B*' layers of the α phase lattice can be presented as a product of two homogeneous transformation matrices. The first one changes the *c* parameter of the transient HCP lattice, $c = 2d_{(111)_\delta} = 2\sqrt{3}a_0/3$, to the *b* parameter of the monoclinic α phase: $c = 2\sqrt{3}a_0/3 \to b$. The corresponding transformation matrix describes a uniaxial contraction, $\hat{\mathbf{A}}(2)$:

$$\hat{\mathbf{A}}(2)_{ij} = \delta_{ij} + \frac{\sqrt{3}b - 2a_0}{2a_0} v_i^{[111]_\delta}\, v_j^{[111]_\delta}. \tag{11}$$

This transformation only changes the interplanar distance of the close-packed layers. It does not deform the unit cell within each layer shown in Fig. 3. The next transformation matrix provides the lattice correspondences (10) in the close-packed planes and describes a planar crystal lattice rearrangement, $\hat{\mathbf{A}}(3)$:

$$\hat{\mathbf{A}}(3)_{ij} = \delta_{ij} + \frac{\sqrt{2}a - 2a_0}{2a_0} v_i^{[\bar{1}10]_\delta}\, v_j^{[\bar{1}10]_\delta} + \frac{\sqrt{6}c\sin\beta - 6a_0}{6a_0} v_i^{[11\bar{2}]_\delta}\, v_j^{[11\bar{2}]_\delta} + \frac{2\sqrt{6}a + 2\sqrt{6}c\sin\beta}{12a_0} v_i^{[\bar{1}10]_\delta}\, v_j^{[11\bar{2}]_\delta}, \tag{12}$$

where $\mathbf{v}^{[\bar{1}10]_\delta}$ and $\mathbf{v}^{[11\bar{2}]_\delta}$ are unit vectors along $[\bar{1}10]_\delta$ and $[11\bar{2}]_\delta$, respectively.

Summarizing the effects of all transformations (7), (11) and (12) produced by shuffling and homogeneous strain, we obtain the total transformation Bain matrix as:

$$\hat{\mathbf{B}} = \hat{\mathbf{A}}(3)\hat{\mathbf{A}}(2)\hat{\mathbf{A}}(1). \tag{13a}$$

Therefore, $\hat{\mathbf{B}}$ is a function of the vector $\bar{\mathbf{h}}$ and the lattice parameters of δ and α phases, $\hat{\mathbf{B}}\left(\bar{\mathbf{h}}, a_0, a, b, c, \beta\right)$. In the coordinate system defined by $x_1 // [\,\bar{1}\,1\,0\,]_\delta$, $x_2 // [\,1\,1\,1\,]_\delta$ and $x_3 // [\,1\,1\,\bar{2}\,]_\delta$, $\hat{\mathbf{B}}$ assumes the form:

$$\hat{\mathbf{B}} = \begin{bmatrix} \dfrac{a}{\sqrt{2}a_0} & \dfrac{\sqrt{3}[a(3\bar{h}_2 - \bar{h}_1) + 2c\cos\beta(\bar{h}_1 + \bar{h}_2)]}{8a_0} & \dfrac{a + 2c\cos\beta}{2\sqrt{6}a_0} \\ 0 & \dfrac{\sqrt{3}b}{2a_0} & 0 \\ 0 & \dfrac{\sqrt{3}c\sin\beta(\bar{h}_1 + \bar{h}_2)}{4a_0} & \dfrac{c\sin\beta}{\sqrt{6}a_0} \end{bmatrix}, \tag{13b}$$

where $\bar{h}_1$ and $\bar{h}_2$ are components of the average displacement vector $\bar{\mathbf{h}} = (\bar{h}_1, \bar{h}_2, \bar{h}_3)_\delta$ defined in Eq. (6) that is confined within the triangle in Fig. 2. In Eq. (13b) the relation $\bar{h}_3 = -\bar{h}_1 - \bar{h}_2$ reflecting the fact that $\bar{\mathbf{h}}$ is in the $(111)_\delta$ plane is used. The correspondence matrix $\hat{\mathbf{C}}$ can be obtained from the lattice relations (8) and (10) as

$$\hat{\mathbf{C}} = \begin{bmatrix} \frac{3\bar{h}_2 - \bar{h}_1}{8} - \frac{5}{12} & \frac{3\bar{h}_2 - \bar{h}_1}{8} + \frac{7}{12} & \frac{3\bar{h}_2 - \bar{h}_1}{8} - \frac{1}{6} \\ \frac{1}{2} & \frac{1}{2} & \frac{1}{2} \\ \frac{\bar{h}_2 + \bar{h}_1}{4} + \frac{1}{6} & \frac{\bar{h}_2 + \bar{h}_1}{4} + \frac{1}{6} & \frac{\bar{h}_2 + \bar{h}_1}{4} - \frac{1}{3} \end{bmatrix}. \tag{14}$$

It determines the lattice correspondence relating the vectors in real and reciprocal spaces in δ parent phase and α phase coordinates:

$$\mathbf{r}_\alpha = \hat{\mathbf{C}}\mathbf{r}_\delta, \qquad \mathbf{H}_\delta = \hat{\mathbf{C}}^{\mathrm{T}}\mathbf{H}_\alpha, \tag{15}$$

where **r** are the crystal lattice site vectors and **H** are reciprocal lattice vectors.

3. Crystallographic Analysis of δ→α Transformation

3.1. Stable Transformation Twin

As $\hat{\mathbf{B}}$ is a function of the vector $\bar{\mathbf{h}}$ and the lattice parameters, a_0, a, b, c and β of the δ and α phases, the twin modes and IPS habit plane orientations are also functions of these variables. In particular, they depend on the vector $\bar{\mathbf{h}}$, which defines the effect of shuffling and is confined inside the triangle in Fig. 2. Each vector $\bar{\mathbf{h}}$ singles out one shuffling mode from multiple possible choices. In general, a procedure to check if a pair of martensite variants satisfies the IPS condition requires a great number of computations because all points in the triangle shown in Fig. 2 should be tested. However, as is shown below, the multiplicity of points $\bar{\mathbf{h}}$ that should normally be tested can be dramatically narrowed if we consider only physically meaningful twins formed by domain pairs. By "physically meaningful twins" we refer to the stable twins whose twin plane and twin shear directions do not change with a variation of the crystal lattice parameters. Therefore, we start with a determination of the stress-accommodating shuffling mode that produces stable twins.

For each $\bar{\mathbf{h}}$ vector in Fig. 2 there are 24 Bain distortion matrices, $\hat{\mathbf{B}}(\nu)$ with $\nu = 1, \ldots, 24$, corresponding to 24 variants of the monoclinic α phase. The orientation relations labeling these Bain matrices are presented in Table A1. These martensite variants provide 23 crystallographically independent pairs of orientation domains, $\hat{\mathbf{B}}(1)\,|\,\hat{\mathbf{B}}(\nu)$ with $\nu = 2, \ldots, 24$. The necessary and sufficient condition for each pair $\hat{\mathbf{B}}(1)\,|\,\hat{\mathbf{B}}(\nu)$ to form a transformation twin is (see [20] for details):

$$\det\left(\left[\hat{\mathbf{B}}(\nu)\,\hat{\mathbf{B}}^{-1}(1)\right]^T\left[\hat{\mathbf{B}}(\nu)\,\hat{\mathbf{B}}^{-1}(1)\right] - \hat{\mathbf{I}}\right) = 0, \tag{16}$$

where det(…) defines the determinant of a matrix, and $I_{ij} = \delta_{ij}$ is a unity matrix. We can find all possible twin pairs among the 23 domain pairs by solving Eq. (16). In general, the twin plane and the twin shear direction of each twin pair are functions of the lattice parameters and $\bar{\mathbf{h}}$ vector.

It has been proved that among all possible twin pairs only three, designated as $\hat{\mathbf{B}}(1)\,|\,\hat{\mathbf{B}}(2)$, $\hat{\mathbf{B}}(1)\,|\,\hat{\mathbf{B}}(4)$ and $\hat{\mathbf{B}}(1)\,|\,\hat{\mathbf{B}}(6)$, are stable twins, which do not depend on the lattice parameters *a*, *b*, *c* and β and thus are not affected by gradual variations of intrinsic crystal lattice parameters. These stable twins can be formed only at the special $\bar{\mathbf{h}}$ points in the triangle shown in Fig. 2 and the locus of these points is the three $<11\bar{2}>_\delta$ directions, as indicated by dashed lines in this figure. The value of each $\bar{\mathbf{h}}$ point on these three directions is designated as

$$\bar{\mathbf{h}} = (\bar{h}_1, \bar{h}_2, \bar{h}_3) = \begin{cases} \rho\dfrac{1}{6}[\bar{2}11] & \text{on DA line} \quad (-0.5 \le \rho \le 1) \quad \text{for } \hat{\mathbf{B}}(1)\,|\,\hat{\mathbf{B}}(4) \\ \rho\dfrac{1}{6}[1\bar{2}1] & \text{on EB line} \quad (-0.5 \le \rho \le 1) \quad \text{for } \hat{\mathbf{B}}(1)\,|\,\hat{\mathbf{B}}(6)\,, \\ \rho\dfrac{1}{6}[11\bar{2}] & \text{on FC line} \quad (-0.5 \le \rho \le 1) \quad \text{for } \hat{\mathbf{B}}(1)\,|\,\hat{\mathbf{B}}(2) \end{cases} \tag{17}$$

where ρ is a parameter characterizing the vector $\bar{\mathbf{h}}$ along $<11\bar{2}>_\delta$. The twin elements of these three stable transformation twins and their corresponding $\bar{\mathbf{h}}$ vectors are listed in Table 1. The numerical values of the twin shear *s* are evaluated with the lattice parameters given in Eq. (9) and are listed in parentheses. It is found that each of the three twins, (K_1, η_1, *s*), is invariant against the variation of ρ. In other words, as long as the $\bar{\mathbf{h}}$ vector stays in its symmetrical direction $<11\bar{2}>_\delta$ the twin is stable. However for its conjugate twin, K_2 changes direction with the value of ρ as $<11\kappa>_\delta$, where $\kappa = (\rho - 4)/(\rho + 2)$ (see Table 1). We call the conjugate twin a "partially stable" twin.

In the case of a phase transformation where the transformation does not involve shuffling, the twin plane and its shear invariancy is with respect to the lattice parameters only. But in the case of plutonium where the transformation involves shuffling, we add one more invariancy with respect to the parameter ρ. As long as $\bar{\mathbf{h}}$ is parallel to a specific symmetrical direction, for example, $<11\bar{2}>_\delta$, the twin plane and its shear direction is invariant with the variation of the displacement magnitude. Therefore the twin is stable as long as the transformation mechanism both preserves the symmetry of the transformation (crystal lattice and shuffling) and allows for variations of the lattice parameters or the shuffling magnitude.

Table 1. Stable transformation twins. $\kappa = (\rho - 4)/(\rho + 2)$

stable twin pair:	twin shear $s = \varepsilon_{\text{twin}}$	$(K_1)_\alpha\ [\eta_1]_\alpha$ $(K_2)_\alpha\ [\eta_2]_\alpha$	$(K_1)_\delta\ [\eta_1]_\delta$ $(K_2)_\delta\ [\eta_2]_\delta$	shuffling $\bar{\mathbf{h}}$

$\hat{\mathbf{B}}(1)\,\|\,\hat{\mathbf{B}}(2)$	$\dfrac{a+2c\cos\beta}{c\sin\beta}$ (0.16015)	$(\bar{2}01)_\alpha\ [102]_\alpha$ $(001)_\alpha\ [\bar{1}00]_\alpha$	$(\bar{1}10)_\delta\ [\bar{1}\,\bar{1}2]_\delta$ $(11\kappa)_\delta [\bar{1}10]_\delta$	$\bar{\mathbf{h}} = \rho\dfrac{1}{6}[11\bar{2}]_\delta$
$\hat{\mathbf{B}}(1)\,\|\,\hat{\mathbf{B}}(4)$	$\dfrac{4ac\cos\beta+15a^2-4c^2}{8ac\sin\beta}$ (0.07529)	$(205)_\alpha\ [\bar{5}02]_\alpha$ $(\bar{2}03)_\alpha\ [302]_\alpha$	$(0\bar{1}1)_\delta\ [\bar{2}11]_\delta$ $(\kappa 11)_\delta\ [0\bar{1}1]_\delta$	$\bar{\mathbf{h}} = \rho\dfrac{1}{6}[\bar{2}11]_\delta$
$\hat{\mathbf{B}}(1)\,\|\,\hat{\mathbf{B}}(6)$	$\dfrac{12ac\cos\beta-7a^2+4c^2}{8ac\sin\beta}$ (0.08486)	$(20\bar{7})_\alpha\ [702]_\alpha$ $(201)_\alpha\ [10\bar{2}]_\alpha$	$(10\bar{1})_\delta\ [1\bar{2}1]_\delta$ $(1\kappa 1)_\delta\ [10\bar{1}]_\delta$	$\bar{\mathbf{h}} = \rho\dfrac{1}{6}[1\bar{2}1]_\delta$

By comparing the Bain distortions generated by the shuffling modes that provide stable transformation twins, it is found that the twin $\hat{\mathbf{B}}(1)\,|\,\hat{\mathbf{B}}(4)$ with a twin plane of $(205)_\alpha$ or $(01\bar{1})_\delta$ is the optimum choice. The selection is made using the following criteria: (1) the minimum typical transformation strain energy, $C_{ijkl}\varepsilon^0_{ij}\varepsilon^0_{kl}$; and (2) the minimum second invariant of the deviartoric strain tensor, $J_2' = \frac{1}{2}(\varepsilon^0_{ij}-\frac{1}{3}\varepsilon^0_{pp}\delta_{ij})(\varepsilon^0_{ij}-\frac{1}{3}\varepsilon^0_{qq}\delta_{ij}) = \frac{1}{6}[(\varepsilon_1-\varepsilon_2)^2+(\varepsilon_2-\varepsilon_3)^2+(\varepsilon_3-\varepsilon_1)^2]$, where ε_1, ε_2 and ε_3 are the principal values of the transformation strain, ε^0_{ij}. Under an isotropic elasticity assumption, the typical strain energy of the martensitic transformation is

$$C_{ijkl}\varepsilon^0_{ij}\varepsilon^0_{kl} = \frac{2\nu\mu}{1-2\nu}(\varepsilon_1+\varepsilon_2+\varepsilon_3)^2 + 2\mu(\varepsilon_1^2+\varepsilon_2^2+\varepsilon_3^2). \qquad (18)$$

Since the transformations with different $\bar{\mathbf{h}}$ involve the same dilatational component, the first term in Eq. (18) is constant for all $\bar{\mathbf{h}}$ and the differences in typical strain energy for different $\bar{\mathbf{h}}$ are fully described by the second term, $(\varepsilon_1^2+\varepsilon_2^2+\varepsilon_3^2)$. Therefore the minimum typical transformation strain energy condition is simplified to $min(\varepsilon_1^2+\varepsilon_2^2+\varepsilon_3^2)$.

The principal values of the transformation deformation are plotted in Fig. 4(a). Figs. 4(b-c) plot $(\varepsilon_1^2+\varepsilon_2^2+\varepsilon_3^2)$ and $(\varepsilon_1-\varepsilon_2)^2+(\varepsilon_2-\varepsilon_3)^2+(\varepsilon_3-\varepsilon_1)^2$, respectively. Figs. 4(b-c) show that the transformation distortion along the DA line, or $[\bar{2}11]_\delta$, is smaller than the other two directions. Thus the shuffling along the DA line is preferred from the aspect of both small transformation strain energy and small deviartoric strain, and the twin $\hat{\mathbf{B}}(1)\,|\,\hat{\mathbf{B}}(4)$ with $(205)_\alpha\ [\bar{5}02]_\alpha$ is the optimum choice among the three stable twins.

Table 1 also shows that among the three possible stable transformation twins, the twin pair of variants 1 and 4 has the smallest twin shear ($\varepsilon_{\text{twin}} = s = 0.07529$). According to the first term in Eq. (3b), this stable twin between variant 1 and 4 is energetically favored over the other two.

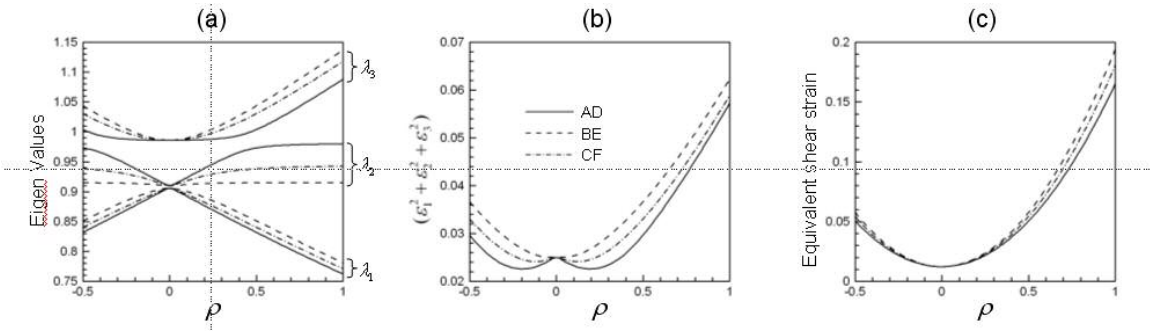

Figure 4. (a) The eigenvalues of the Hermitian part of the Bain distortions, (b) $(\varepsilon_1^2+\varepsilon_2^2+\varepsilon_3^2)$ and (c) $(\varepsilon_1-\varepsilon_2)^2+(\varepsilon_2-\varepsilon_3)^2+(\varepsilon_3-\varepsilon_1)^2$ along DA, EB, and FC, respectively.

As will be shown later, the selection of the 1-4 twin pair over the other two pairs is a result of the more important consideration — the IPS requirement: the 1-2 and 1-6 twin pairs cannot provide IPS.

It should be mentioned that these three stable transformation twins are also favored over other twins, not only from a stability point of view, but also from energetic considerations: they have the lowest twin boundary energy. Indeed, in general, the shuffling involved in the transformation produces partial dislocations at twin boundaries. It can be shown that only these three stable twins can achieve a dislocation-free fit along twin boundaries, and thus eliminate the energy associated with partial dislocations.

The experimental observations in [10] fully support the predicted stable transformation twin formed by alternating domains of variants 1 and 4 and with $(205)_\alpha$ twin planes. Our $(205)_\alpha$ twin between variants 1 and 4 predicts that these two variants share a parallel $[020]_\alpha$ direction, that their *a* axis directions are along $[\bar{1}10]_\delta$ and $[\bar{1}01]_\delta$, respectively, and that the twin plane is co-planar with $(01\bar{1})_\delta$. This prediction is confirmed by the observations in [12].

3.2. Invariant Plane Strain

It has been shown that the search is narrowed down to $(205)_\alpha$ twins between variants 1 and 4, which is the energetically preferred stable transformation twin provided by the special vectors $\bar{\mathbf{h}} = \rho/6[\bar{2}11]_\delta$ with ρ varying in the range $(-0.5 \le \rho \le 1)$. To determine the Bain distortion of the $\delta \rightarrow \alpha$ transformation, we have to determine the optimal shuffling mode, i.e., the best choice for the parameter ρ $(-0.5 \le \rho \le 1)$. This further screening process is done by using the first criterion, the IPS condition.

As discussed in Section 1.2, to provide IPS, the domain-averaged transformation matrix $<\hat{\mathbf{A}}>$ (Eq. (5)) has to be reduced to the form $<\hat{\mathbf{A}}>_{ij} = \delta_{ij} + \varepsilon\, l_i n_j$. The necessary and sufficient condition for $<\hat{\mathbf{A}}>$ to provide IPS is (again, see [20] for details) is:

$$\overline{\lambda}_1 \le 1, \quad \overline{\lambda}_2 = 1, \quad \text{and} \quad \overline{\lambda}_3 \ge 1, \tag{19}$$

where $\overline{\lambda}_i$ are the eigenvalues of the Hermitian part of the matrix $<\hat{\mathbf{A}}>$. (The Hermitian part of a matrix is the matrix excluding the unitary part in its polar decomposition.) The equation

$$\overline{\lambda}_2(x,\rho) = 1 \tag{20}$$

is a necessary condition for the IPS. For each parameter ρ (vector $\overline{\mathbf{h}}$), we have to find a special value of the domain volume fraction *x* that provides Eq. (20).

The normal to the invariant habit plane, $\mathbf{n}$, and the IPS shear vector, $\varepsilon\mathbf{l}$, are determined by the equations

$$\mathbf{n} = \sqrt{\frac{\overline{\lambda}_3^2 - 1}{\overline{\lambda}_3^2 - \overline{\lambda}_1^2}}\mathbf{e}_3 \pm \sqrt{\frac{1 - \overline{\lambda}_1^2}{\overline{\lambda}_3^2 - \overline{\lambda}_1^2}}\mathbf{e}_1 \tag{21}$$

and

$$\varepsilon\mathbf{l} = (\lambda_3 - \lambda_1)\left(\overline{\lambda}_1\sqrt{\frac{\overline{\lambda}_3^2 - 1}{\overline{\lambda}_3^2 - \overline{\lambda}_1^2}}\mathbf{e}_3 \mp \overline{\lambda}_3\sqrt{\frac{1 - \overline{\lambda}_1^2}{\overline{\lambda}_3^2 - \overline{\lambda}_1^2}}\mathbf{e}_1\right), \tag{22}$$

where $\mathbf{e}_1$ and $\mathbf{e}_3$ are unit eigenvectors of the matrix $<\hat{\mathbf{A}}^T(x,\rho)><\hat{\mathbf{A}}(x,\rho)>$ corresponding to the eigenvalues $\overline{\lambda}_1$ and $\overline{\lambda}_3$ at $\overline{\lambda}_2(x,\rho) = 1$ [19, 20]. As follows from Eqs. (21) and (22), in general, there are two IPS solutions for a given transformation deformation.

The orientation relations between the parent and product phases of the $\delta\rightarrow\alpha$ transformation are characterized by both the correspondence matrix $\hat{\mathbf{C}}$ and the transformation distortion matrix $\hat{\mathbf{A}}$. The angle between vectors $\mathbf{r}_\delta$ in the parent phase and $\mathbf{r}_\alpha$ in the martensite phase is given by

$$\langle \mathbf{r}_\delta, \mathbf{r}_\alpha \rangle = \cos^{-1}\left(\frac{\mathbf{r}_\delta \cdot \hat{\mathbf{A}}\hat{\mathbf{C}}^{-1}\mathbf{r}_\alpha}{|\mathbf{r}_\delta||\hat{\mathbf{A}}\hat{\mathbf{C}}^{-1}\mathbf{r}_\alpha|}\right), \tag{23a}$$

The angle between a plane in the parent δ phase normal to its reciprocal lattice vector, $\mathbf{H}_\delta$, and a plane in the α phase normal to its reciprocal lattice vector, $\mathbf{H}_\alpha$, is given by

$$\langle \mathbf{H}_\delta, \mathbf{H}_\alpha \rangle = \cos^{-1}\left(\frac{\mathbf{H}_\delta \cdot \hat{\mathbf{A}}^{-\mathrm{T}}\hat{\mathbf{C}}^{\mathrm{T}}\mathbf{H}_\alpha}{|\mathbf{H}_\delta||\hat{\mathbf{A}}^{-\mathrm{T}}\hat{\mathbf{C}}^{\mathrm{T}}\mathbf{H}_\alpha|}\right). \tag{23b}$$

$\hat{\mathbf{A}} = \hat{\mathbf{R}}_{\text{plate}}\hat{\mathbf{B}}(1)$ for variant 1, and, $\hat{\mathbf{A}} = \hat{\mathbf{R}}_{\text{plate}}\hat{\mathbf{R}}_{\text{twin}}\hat{\mathbf{B}}(1)$ for variant 2, where $\hat{\mathbf{R}}_{\text{plate}}$ and $\hat{\mathbf{R}}_{\text{twin}}$ are defined in Eq. (5).

Eqs. (20)-(23) solve the problem of the crystallography of the martensitic transformation if we know the lattice correspondence and the values of the crystal lattice parameters of the α and δ phases at the composition and temperature of the transformation. Unfortunately, the literature shows that both the lattice correspondence

and the accurate crystal lattice parameters for the δ→α transformation in the plutonium alloys are not well known.

3.3. Dependence of Crystallography on Volume Effect of Transformation

The normal to the invariant habit plane, **n**, is very sensitive to the lattice parameters, a_0, a, b, c and β, and especially to the ratio of the unit cell volumes of the phases, $\chi = V_\alpha / V_\delta = (abc\sin\beta)/(16a_0^3)$. The value χ depends on the composition of the plutonium alloys, the temperature, and other factors. It is shown in the Discussion that the real ratio χ may deviate considerably from the reference value χ_0 calculated by using the data in Eq. (9). We will characterize these deviations by the dilatation parameter $\delta = \sqrt[3]{\chi/\chi_0}$, which, in fact, is an uncertainty parameter reflecting an incompleteness or inaccuracy of the available experimental data on the crystal lattice parameters of the α and δ phases at the temperature and composition of transformation. For the plutonium alloys studied in this paper, the deviation of δ from 1 should be a physically reasonable value. Our calculation shows that the only stable twin mode providing IPS within this range of the parameter δ is the stable $(205)_\alpha\,[\bar{5}02]_\alpha$ twin, with $\delta \geq 1.019$ ($V_\alpha/V_\delta \geq 0.860$). The other two stable twins, $(\bar{2}01)_\alpha\,[102]_\alpha$ and $(20\bar{7})_\alpha\,[702]_\alpha$ (see Table 1), can provide IPS only with $\delta \geq 1.059$ ($V_\alpha/V_\delta \geq 0.965$) and $\delta \geq 1.092$ ($V_\alpha/V_\delta \geq 1.058$), respectively, which are both too large to be explained by inaccuracies in the crystal lattice parameter data.

3.4. Possible Invariant Plane Strain Solutions

For given δ and $\bar{\mathbf{h}}$ vectors ($-0.5 \leq \rho \leq 1$), the crystallographic calculation of IPS can be carried out to check if an IPS can be attained at any value of the volume fraction x and thus to obtain the invariant plane habit orientation **n**=**n**(δ,ρ) and x=x(δ,ρ) with $0 \leq x \leq 1$. However, since the exact value of the δ parameter is unknown, we will address the IPS problem differently. We will find the values of the parameter δ providing the IPS solution at different values of ρ and x and consider only those values of δ that are within a physically meaningful range, $1<\delta<1.025$ (from -18.7% to -12.5% volume change). This procedure considerably narrows the scope of the possible crystallographic mechanisms of the transformation. The next constraint on the IPS solutions is imposed by the observed orientation relations. The experiments reveal the parallelisms, $[\bar{1}10]_\delta \parallel [100]_\alpha$ and $(111)_\delta \parallel (020)_\alpha$, within the range of $\pm 5^\circ \sim 7^\circ$ [2, 9]. Therefore, the range of the IPS solutions can be narrowed further by calculating the orientation relations by using Eq. (23) and rejecting the IPS solutions that result in a deviation of the calculated orientation relations from the $[\bar{1}10]_\delta \parallel [100]_\alpha$ and $(111)_\delta \parallel (020)_\alpha$ larger than the observed deviations.

Fig. 5(a) presents a plot of the dilatation parameter $\delta = \delta(\rho, x)$ providing an IPS. The variation range of δ at a given value ρ (for all possible x) is plotted in Fig. 5(b). We discard solutions that require $\delta > 1.025$ (above the dashed line in Fig. 5(b),

corresponding to $V_\alpha/V_\delta > 0.875$). The regions corresponding to physically acceptable solutions, ($\delta(\rho,x) \le 1.025$) are bounded by dashed lines and highlighted by color contour plots in Fig. 5(a), where $\delta(\rho,x)$ assumes a constant value at each contour line.

Fig. 6 presents a plot of the shear component $\varepsilon_s = \varepsilon_s(\rho,x)$ of the IPS strain ε (see Eq. (2b)). The solutions corresponding to $\delta(\rho,x) \le 1.025$ are bounded by dashed lines. The contour lines of $\delta(\rho,x)$ corresponding to that in Fig. 5(a) are also shown. Two points, (ρ = -0.42, x = 0.5) and (ρ = 0.42, x = 0.5), can be singled out for their minimum value ε_s = 0.0126. The shuffling mechanism corresponding to ρ = -0.42 is close to $(m_1\ m_2\ m_3)$=(1 9 9). The orientation of the invariant habit plane of a martensite plate provided by this solution is **n** = (0.1718, -0.6613, -0.7302). The orientation relations corresponding to this solution provides the deviations from $[\bar{1}10]_\delta \parallel [100]_\alpha$ and $(111)_\delta \parallel (020)_\alpha$ within the observed range [2, 9]: the calculated angle between the $[100]_\alpha$ and $[\bar{1}10]_\delta$ directions is 3.65° for the first IPS solution (4.08° for the second IPS solution), whereas the calculated angle between the predicted $(020)_\alpha$ and $(111)_\delta$ planes is 4.28° for both IPS solutions. The shuffling mechanism corresponding to ρ = 0.42 is close to $(m_1\ m_2\ m_3)$=(16 5 5). The corresponding habit plane orientation of IPS is **n** = (0.9849, -0.0830, 0.1518). The deviations from the nominal orientation relations ($[\bar{1}10]_\delta \parallel [100]_\alpha$ and $(111)_\delta \parallel (020)_\alpha$) are the same as the case of ρ = -0.42.

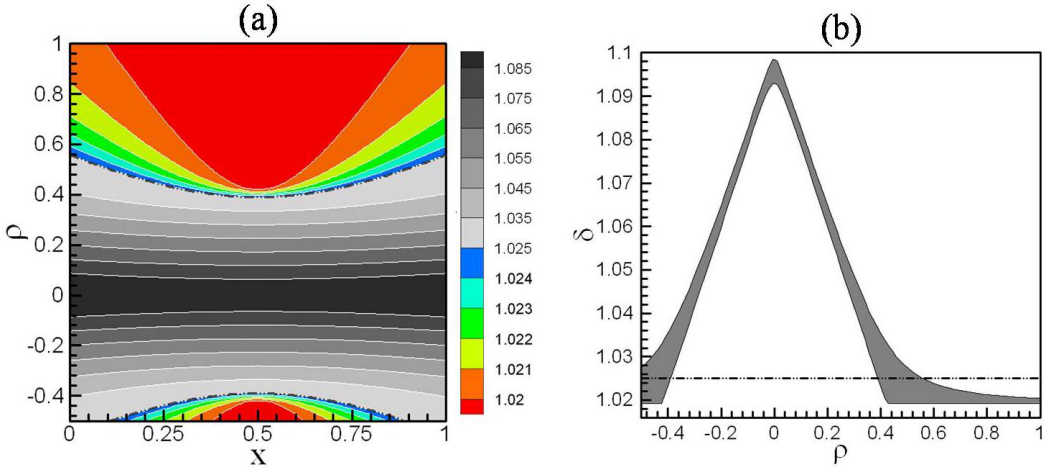

Figure 5. (a) Contour plot of the dilatation parameter $\delta = \delta(\rho,x)$ that provides IPS at each set of ρ and x. (b) The variation range of parameter δ at given value ρ (for all possible x). The physically possible solutions $\delta(\rho,x) \le 1.025$ are highlighted by color contour plots in (a) and bounded by dashed line in (a) and (b).

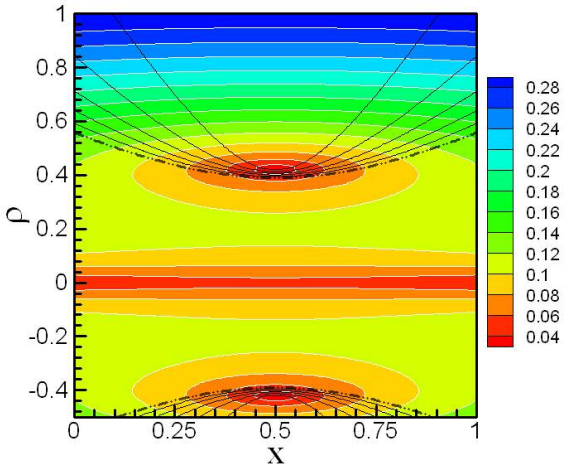

Figure 6. Contour plot of the shear component $\varepsilon_s = \varepsilon_s(\rho, x)$ of the shape strain ε of the IPS at each set of ρ and x (see Eq. (2b)). The physically possible solutions (corresponding to $\delta(\rho, x) \le 1.025$ in Fig. 5) are bounded by dashed lines. The contour lines of constant δ values (corresponding to that in Fig. 5(a)) are also shown.

The IPS solutions of the habit plane normal directions are obtained for all possible $\bar{\mathbf{h}}$ vectors ($-0.5 \le \rho \le 1$) providing the stable $(205)_\alpha$ transformation twin. In Fig. 7 we plot only the habit plane orientations **n** of IPS corresponding to $\delta(\rho, x) \le 1.025$ and orientation relations within 5° from $[\bar{1}10]_\delta \parallel [100]_\alpha$ and $(111)_\delta \parallel (020)_\alpha$. The symbols "×" indicate the experimentally observed $\{123\}_\delta$, $\{112\}_\delta$ and $\{223\}_\delta$ habit planes [10, 12, 13]. The IPS solutions are plotted in different colors according to the dilatation parameter δ. Figure 7 shows how sensitive the invariant plane normal is to the value of the parameter δ. To provide information on the domain volume fraction x, we highlight the solutions corresponding to several constant x values.

Figures 5, 6 and 7 summarize all the information on the orientation relations and corresponding habit planes that we have obtained from the possible IPS solutions and crystallographic mechanisms that provide for a stable $(205)_\alpha [\bar{5}02]_\alpha$ stress-accommodating twin.

The prediction of the morphology of the martensitic transformation could be unambiguous if we had accurate data on the crystal lattice parameters and use the minimum strain energy criterion. However, Figs. 5-7 allow one to get this information even if the available data are either incomplete or inaccurate. For example, if accurate experimental data on the crystal lattice parameters (value δ) and on the volume fraction of twins, x, are available, the diagrams shown in Figs. 5-7 determine the shuffling mode ρ, the IPS, and the habit plane orientation. Or, if the habit normal direction and the volume fraction x are measured, the value of parameter δ and the shuffling mode can be obtained.

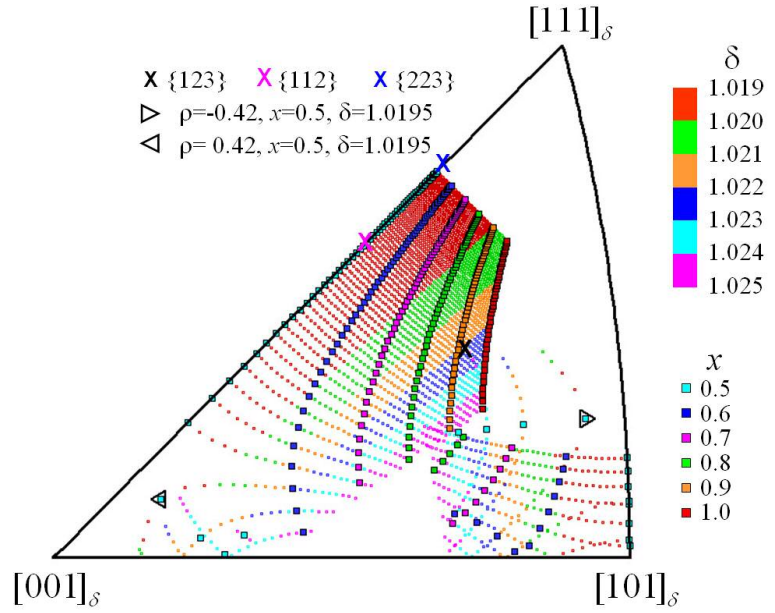

Figure 7. The stereographic projections of all possible IPS habit plane orientations provided by the most stable transformation twin, i.e., $(205)_\alpha$ twin between variants 1 and 4.

With the currently available experimental data, the value of the parameter δ can be estimated only within a range ($1 \le \delta \le 1.025$), and there are only two direct experimental reports on the habit plane orientations. The first reports the habit plane close to $\{123\}_\delta$ [10], and the second reports habit plane characterized by a point within the area between $\{112\}_\delta$, $\{223\}_\delta$ and $\{123\}_\delta$ on the stereographic projection plot [12, 13]. Recent analysis also offered indirect evidence of a {111} habit plane [12, 13].

In spite of the limited information and uncertainties mentioned above, the theory predicts that the transformation twins involved in the martensitic transformation should be $(205)_\alpha\ [\bar{5}02]_\alpha$ stable twins. Under these assumptions, all possible IPS solutions consistent with the limited experimental data have been found.

Among all possible shuffling modes, there are two simplest modes of shortest period, namely double and single elementary shuffling modes corresponding to points "D" and "A" in Fig. 2, respectively. For point "D", its $\bar{\mathbf{h}}$ vector characterizes a double elementary shuffling, $(m_1\ m_2\ m_3)$=(0 1 1), consisting of double partial δ lattice translation vectors $1/6[1\,\bar{2}\,1]_\delta$ and $1/6[1\,1\,\bar{2}]_\delta$ with a period of four $(111)_\delta$ layers. The shuffling corresponding to the point "A" is produced by $(m_1\ m_2\ m_3)$ =(1 0 0). It is a single elementary shuffling resulting in only $1/6[\bar{2}\,1\,1]_\delta$ partial δ lattice translations with a period of two $(111)_\delta$ layers. It should be noted that this single elementary shuffling mechanism has been extensively studied [2, 6, 7, 10] under the name "correspondence III" first used in [2]. The complete IPS solutions of these two simplest shuffling modes are presented below.

3.5. Double Elementary Shuffling

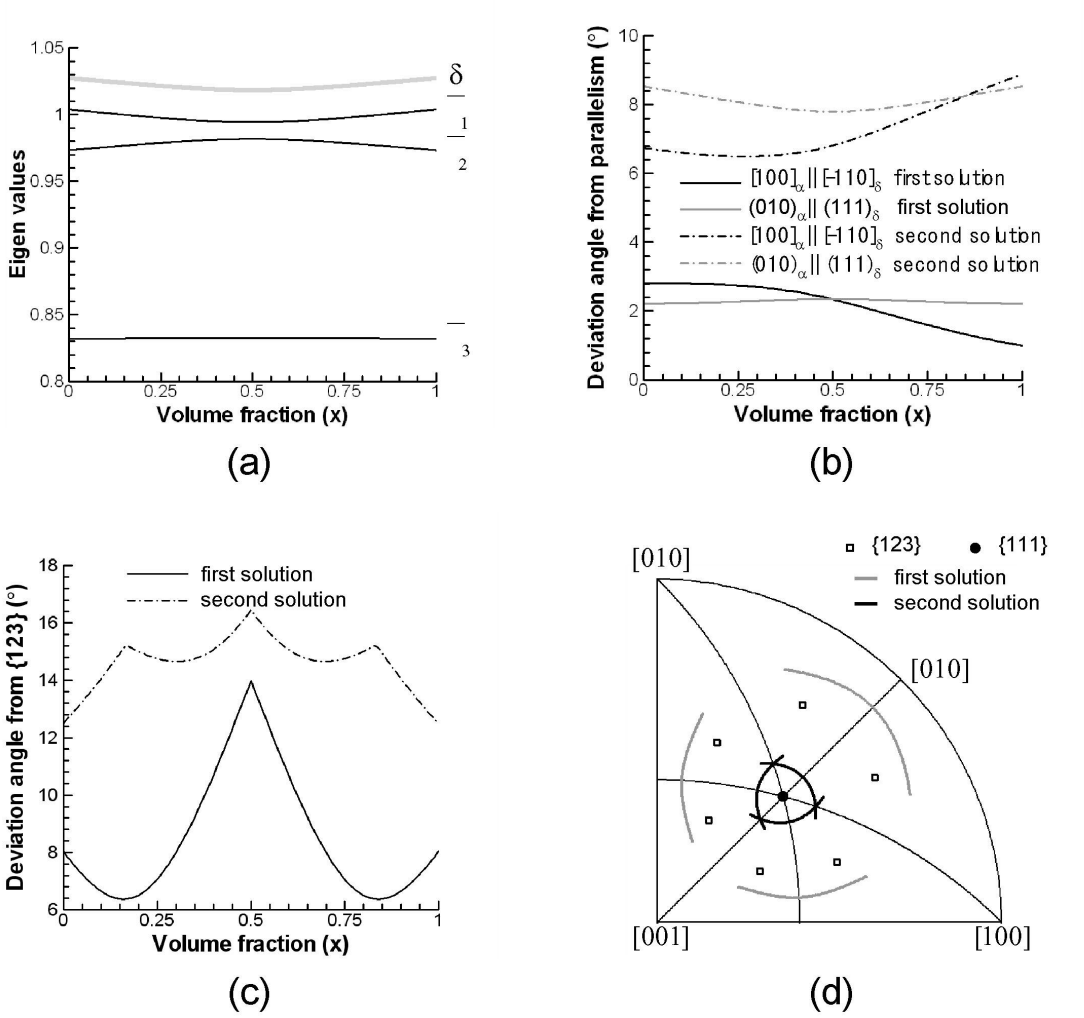

Figure 8. (a) The eigenvalues of the Hermitian part of the domain-averaged transformation matrix $<\hat{\mathbf{A}}>$ and the dilatation parameter δ versus domain volume fraction x for double elementary shuffling mode. (b) The deviations from $[100]_\alpha \,||\, [\bar{1}10]_\delta$ and $(010)_\alpha \,||\, (111)_\delta$. (c) The deviation of the IPS habit plane normal direction from $\{123\}_\delta$ versus domain volume fraction x. (d) The stereographic projections of the IPS habit plane normal directions for all possible domain volume fraction x. They are clustered around $\{123\}_\delta$ and $\{111\}_\delta$, respectively.

For the double elementary shuffling mode, which is characterized by ρ = -0.5 ($\bar{\mathbf{h}} = 1/12\left[2\,\bar{1}\,\bar{1}\right]$) corresponding to point "D" in Fig. 2, we plot in Fig. 8(a) the eigenvalues, $\bar{\lambda}_i$, of the Hermitian part of the domain-averaged transformation matrix $<\hat{\mathbf{A}}>$ versus domain volume fraction x and the corresponding dilatation parameter δ. The value of δ varies from 1.019 to 1.027. If the real δ value is known, we can determine the volume fraction x and the IPS habit plane orientation.

To be mentioned is that there are always two IPS solutions for each set of (x, ρ) (see Eqs. (21) and (22)). Two solutions of the invariant plane normal direction can be obtained by Eq. (21). Eqs. (21), (22), (5), (23a) and (23b) all together give two solutions of the orientation relations. These two solutions are called first and second solution for convenience. It is found that the gradual change of the dilatation parameter δ (or equivalently x) leads to a continuous change in its IPS solutions. The two IPS solutions of the invariant strain normal direction and the orientation relations versus x value are shown in Fig. 8(b-d).

The calculations are compared with the experimentally observed orientation relations, $[100]_\alpha \| [\bar{1}10]_\delta$ and $(010)_\alpha \| (111)_\delta$, in Fig. 8(b). It plots the deviation angles of the $[100]_\alpha$ direction and $(010)_\alpha$ plane from the $[\bar{1}10]_\delta$ direction and $(111)_\delta$ plane. The first solution is close to the $[100]_\alpha \| [\bar{1}10]_\delta$ and $(010)_\alpha \| (111)_\delta$ orientation relations with deviation angles smaller than 2.8° for all x value. The second solution deviates from the parallelisms by 6.5°~8.9°.

The calculated orientations of all invariant habit planes for all possible domain volume fraction $0 \le x \le 1$ are plotted on the stereographic projections in Fig. 8(d). Fig. 8(c) plots the deviation angle of the invariant plane normal direction from the experimentally observed $\{123\}_\delta$ direction. The first solution gives the invariant plane close to $\{123\}_\delta$ with deviation angle of 6.4°~14.0°. The best fit (6.37°) is obtained with the volume fraction x=0.16 (see Fig. 8(c)). The corresponding dilatation parameter δ=1.0239 (see Fig. 7(a)). The stereographic projection in Fig. 8(d) clearly shows the first solution around $\{123\}_\delta$. It also shows the second solution around $\{111\}_\delta$. Its deviation angle from $\{111\}_\delta$ is 7.1°~10.2°. The best fit (7.07°) is obtained at x=0.5 with δ=1.0192. In both cases, the required dilatation parameter is δ≈1.02. Both IPS solutions yield the shape strain $\varepsilon \approx 0.17$.

3.6. Single Elementary Shuffling

For the single elementary shuffling mode, which is characterized by ρ = 1 ($\bar{\mathbf{h}} = 1/6[\bar{2}11]$) corresponding to point "A" in Fig. 2, the eigenvalues $\bar{\lambda}_i$ and dilatation parameter δ are plotted in Fig. 9(a). It shows that $\bar{\lambda}_i$ practically does not depend on x. The δ value also varies very little for the whole range $0 \le x \le 1$ (δ = 1.019~1.020).

The first solution gives a good agreement with experimentally observed orientation relations: the deviation angles are smaller than 1.7° for all x value. The second solution does not provide such orientation relations: the deviation angles are greater than 16.3°, and thus should be rejected as a possible solution of the MT mechanism.

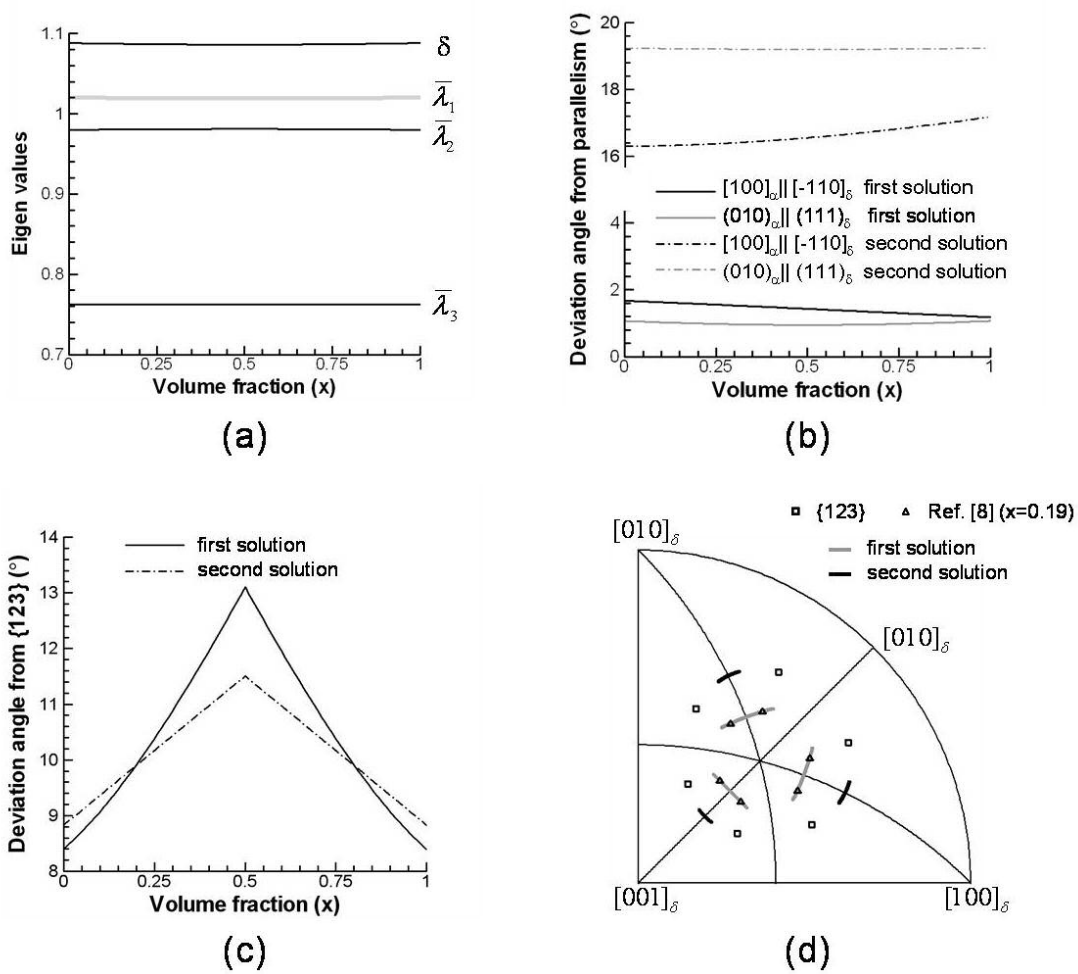

Figure 9. (a) The eigenvalues of the Hermitian part of the domain-averaged transformation matrix $<\hat{\mathbf{A}}>$ and the dilatation parameter δ versus domain volume fraction x for single elementary shuffling mode. (b) The deviations from the parallelisms $[100]_\alpha \parallel [-110]_\delta$ and $(010)_\alpha \parallel (111)_\delta$. (c) The deviation of the invariant plane normal direction from $\{123\}_\delta$ versus domain volume fraction x. (d) The stereographic projections of the invariant plane normal directions for all possible domain volume fraction x.

The calculated poles of the invariant planes for all possible domain volume fractions $0 \le x \le 1$ are shown at stereographic projections in Fig. 9(d). Fig. 9(c) plots the deviation angle of the invariant plane normal direction from the $\{123\}_\delta$ direction. The best fit (8.40°) is obtained for the first solution at x=0 or 1. The corresponding dilatation parameter δ = 1.0204 (see Fig. 9(a)). This IPS solution yields the shape strain $\varepsilon \approx 0.33$. This solution corresponds to a single domain (untwinned) martensitic plate with the invariant habit plane, which is not observed.

4. Discussion

There are experimental observations of the orientation relations, transformation twins and habit plane normal directions. The observations indicate that orientation relations are close to $[\bar{1}10]_\delta \parallel [100]_\alpha$ and $(111)_\delta \parallel (020)_\alpha$ within an accuracy of $\pm 5^\circ \sim 7^\circ$ [2, 9].

Observations of the regular striations of martensite plates attributed to the $(205)_\alpha$ twin boundaries have been reported [10, 12]. The observed habit planes are close to $\{123\}_\delta$ [10]. In an absence of accurate crystal lattice parameter measurement for the states where the martensitic structures have been observed, we used these observations as a criterion for a choice of the crystal lattice rearrangement mechanism. Although the crystallographic analysis on twin modes has been presented in a number of papers, they are still insufficient to fully explain the observation results. The MT mechanism proposed by Zocco et al. predicts the habit plane orientation close to $\{123\}_\delta$ [10]. However, this prediction is based on a consideration of a limited number of possible crystal lattice rearrangements. The theory presented in this study selects the crystal lattice rearrangement mechanism considering a significantly wider pool of transformation options.

It is shown that the orientation of the invariant plane of a multi-domain martensite plate is very sensitive to the values of the crystal lattice parameters and, in particular, to the volume change in the MT. Given the fact that the lattice parameters of Pu-Ga alloys significantly depend on the gallium concentration, temperature, and heat treatment procedure [11, 14-18], any theoretical predictions based on the IPS theory require very accurate measurements of the crystal lattice parameters at the states where the microstructure is formed. The existing data on the plutonium MT do not provide this accuracy.

The dependence of the lattice parameters of the FCC δ phase on gallium concentration and transformation temperature can be estimated by extrapolating the published data in Fig. 2 of [16]. It is more difficult to estimate the values of the lattice parameters for the α phase. Fig. 11 of [15] shows that the MT produces the volume change of −20.1% for pure plutonium and −15.9% for Pu-3.4%Ga alloy, but no temperature information is provided. The volume change corresponding to the parameters (9) that are reported in [10] is −18.7%. These data are used here as a reference state corresponding $\delta = 1$. The situation is further complicated by the fact that the MT in Pu-Ga alloys produces the α′ rather than the α phase. The α′ phase is an expanded α phase with trapped gallium in its substitutional lattice sites [15]. The α′ phase is unstable and undergoes nanoscale ordering and also changes the composition at even comparatively low temperature, which lead to the change of lattice expansion [15]. Thus the lattice parameters of α′ phase are very sensitive to the sample history (pressure, heat treatment regime, etc.). For example, its volume can decrease during annealing at moderate temperatures (25-70ºC) [18]. It is usually assumed that the axial ratios of the monoclinic α′ phase are the same as those of the α phase. Experimental measurements for several different gallium concentrations in Fig. 32 of [18] shows that such assumption seems reasonable.

Ref. 10 gave the first direct evidence of transformation twins within α phase plates based on the TEM, electron diffraction, and a crystallographic analysis. The values of the lattice parameters were obtained with a $\delta \rightarrow \alpha$ volume change of −18.7% by assuming the same axial ratios of the monoclinic α structure as those for the pure plutonium system

[10]. Recently, it has been pointed out [15, 18] that the alloy used in [10] was Pu-3.4%Ga alloy.

Several other factors also affect the lattice parameters [15]. One is the heterogeneous Ga distribution formed as a result of diffusion from α′ phase to the surrounding δ phase. (These heterogeneities will cause variations in the lattice parameters of both the α′ and δ phases [16].) The other factors are the ordering of gallium in the α′ phase [25], which relaxes the lattice expansion, and the formation of vacancies or vacancy clusters due to self-irradiation damage. To take into account this uncertainty in volume change, we have used the dilatation parameter δ characterizing the relative deviation of the transformation-induced volume change with respect to that of the "standard reference state" characterized by the most recent crystal lattice parameters (9) taken from [10]. Using these data makes it possible to compare our results with those obtained in [10]. In this paper we set a limit range of $1 \le \delta \le 1.025$ (from -18.7% to -12.5% volume change) that, we believe, covers the physically possible value for $\delta \rightarrow \alpha$ MT.

In this paper, we considered all possible transformation mechanisms associated with twin formation and shuffling of close-packed $(111)_\delta$ layers in the FCC δ phase lattice during the transformation. Since the invariant plane orientations, and even the existence of IPS, are very sensitive to the volume change of MT, it is not feasible to directly search for the twin pair that provides an IPS, as is conventionally done when the crystallographic data are accurately determined. Instead, we first search for the transformation twin mode because transformation twins do not depend on the transformation volume change, which is the main uncertainty factor. To determine the twin mode, we analyze all twin-related pairs formed by the 24 variants of α phase structural domains with the Bain distortion produced by all possible shuffling modes.

As a result of this search, we found three pairs of twin-related domains that can produce the stable transformation twins. Unlike other possible twins, the orientation of the twin plane of the stable twins is fixed, i.e., it does not change gradually upon gradual changes of the crystal lattice parameters with the alloy concentration. There is also an energy argument in favor of the stable twins: only the stable transformation twins can form low energy dislocation-free twin boundaries despite of the generation of partial dislocations associated with the transformation shuffling. All other twin boundaries would be decorated by ultra-dense distribution of partial dislocations. Therefore, the twin boundaries of these three stable twins should have the lowest twin boundary energy. Among these three stable twins, the $(205)_\alpha$ twin is selected because it is the only stable twin that can produce the IPS. The $(205)_\alpha$ twin also has a smaller transformation strain energy and a smaller deviatoric strain than the other two stable twins. This prediction is fully supported by experimental observations.

By taking into account the uncertainty in volume change, we found all possible orientations of invariant planes for the MT involving $(205)_\alpha$ stress-accommodating twinning. All possible IPS solutions at $\delta(\rho, x) \le 1.025$, which give the orientation

relations close to $[100]_\alpha \parallel [\bar{1}10]_\delta$ and $(010)_\alpha \parallel (111)_\delta$ (deviation less than 5°), are presented. These results provide a set of possible solutions. To find which of them corresponds to the transformation mode for a given system, more accurate measurements of the crystal lattice parameters for this specific system is required.

A lack of experimental measurements disallows a decisive selection of shuffling parameter ρ for $(205)_\alpha [\bar{5}02]_\alpha$ stable twins. Under such circumstance, two special shuffling modes are chosen to describe possible MT mechanisms; their IPS solutions are presented in detail. They are the simplest shuffling modes of the shortest period, single and double elementary shuffling modes. In terms of Eq. (6), they correspond to $(m_1\ m_2\ m_3)$=(1 0 0) and $(m_1\ m_2\ m_3)$=(0 1 1), respectively.

It is worth noting that the shuffling that involves a long period could be also studied by considering the closest short-period simple elementary shuffling mode. For example, the shuffling of $(m_1\ m_2\ m_3)$=(1 9 9) that produces the minimum shear strain, in fact, is a faulted double elementary shuffling $(m_1\ m_2\ m_3)$=(0 1 1) with "shuffling fault" repeating every 38 $(111)_\delta$ layers; its general behavior could be understood based on the behavior of the double elementary shuffling mechanism. Thus simple shuffling modes are representative of a larger pool of shuffling mechanisms and chosen for further investigation.

The double elementary shuffling mode corresponding to $(m_1\ m_2\ m_3)$=(0 1 1) could be one of the optimum modes. The predicted habit planes calculated with the use of this mode are in agreement with the experimental observation. They are close to the observed $\{123\}_\delta$ with deviation angle of 6.4°~14.0°. The best fit (6.37°) is obtained at x=0.16. It yields IPS shape strain $\varepsilon \approx 0.17$. The required dilatation parameter $\delta \approx 1.02$, which is within the acceptable range.

An alternative simple mechanism is a single elementary shuffling (in fact, it was also studied in [10]). Our analysis predicts the IPS habit planes close to $\{123\}_\delta$ with a deviation angle of 8.4°~13.1° . The solution obtained in [10] also follows from our analysis and is highlighted in Fig. 9(d). However, the best fit (8.4° deviation) for a single elementary shuffling is obtained not for the solution in [10] involving the $(205)_\alpha$ twinning but for a single-domain plate that has no accommodation twins at all (x=0). It yields IPS shape strain $\varepsilon \approx 0.33$. The required dilatation parameter is $\delta \approx 1.02$. This single-domain solution would be more preferable than the multi-twin solution obtained in [10] because the former has a lower strain energy: the twinned IPS plate considered in [10] always has a higher strain energy than a single-domain IPS plate with the same habit plane. However, most of α martensitic plates seem to contain transformation-induced twins. If this observation is accurate, the mechanism based on a single elementary shuffling should be rejected.

It should be emphasized that the shuffling involved in MT process adds additional configurational degrees of freedom and thus considerably complicates the

crystallographic analysis because, in general, it generates partial dislocations at the boundaries of twin-related domains.

Both the MT mechanisms which involve single and double elementary shuffling modes require a dilatation parameter $\delta \approx 1.02$. This corresponds to a ~6% larger volume unit cell of the α phase than that determined by the parameters (9). Given the uncertainty in the determination of the lattice parameters discussed above, $\delta \approx 1.02$ is a reasonable number.

To provide more insight into the effect of δ, we also present the calculation result with δ=1, i.e., assuming the lattice parameters given in Eq. (9) be accurate. In particular, we carry out the crystallographic analysis for 7 simplest shuffling modes corresponding to a single shuffling (points "A", "B", "C"), double shuffling ("D", "E", "F") and triple shuffling ("O") in Fig. 2. In fact, four of the above shuffling mechanisms have been extensively studied [2, 6, 7, 10] under the names first used in Ref. 2: correspondence I ("C"), correspondence II ("B"), correspondence III ("A"), and correspondence IV ("O"). In Table A2 we list the transformation matrices produced by these 7 shuffling modes, which can be obtained by substituting the corresponding $\bar{\mathbf{h}}$ vectors (6) and crystallographic data (9) into Eq. (13). The transformation matrices are given for convenience in both the coordinate system defined by $x_1 // [\bar{1}10]_\delta$, $x_2 // [111]_\delta$, $x_3 // [11\bar{2}]_\delta$ and the conventional coordinate system described by the cubic axes of the FCC δ phase. The corresponding eigenvalues are also listed there. In Table A1, we list the 24 variants of the α phase. It is found that the double ("D", "E", "F") and triple ("O") shuffling modes cannot provide IPS with δ=1. There are 5 twin pairs involving single shuffling modes ("A", "B", "C") that provide 14 IPS solutions. They are listed in Table A3 and numbered 1, …, 14. The stereographic projections of the normal directions of the 14 invariant planes are plotted in Fig. A1(a) of Appendix. Their deviation angles from $\{123\}_\delta$ are plotted in Fig. A1(b). As shown in Fig. A1, some of the 14 invariant planes are very close to the experimentally observed $\{123\}_\delta$, e.g., No. 1 and No. 3 invariant planes deviate from $\{123\}_\delta$ direction by 1.192^o and 2.203^o, respectively. However, none of the 5 twin pairs that provide IPS in Table A3 coincide with the experimentally observed $(205)_\alpha$ twin. These facts indicate that unless the crystal lattice parameters of the α and δ phases in the observed microstructure deviate from the parameters in Eq. (9) corresponding to δ=1, and thus $\delta \neq 1$, the strain-accommodation leads to an apparent contradiction with experimental observation.

5. Conclusion

The crystallographic analysis of MT mechanisms of the δ→α transformation takes into account several factors. They are the layered character of the crystal structure of the α phase, its susceptibility to a formation of stacking faults, possible uncertainty in a determination of the transformation volume change, and the strain energy minimization condition. It is shown that a requirement of the stability of transformation twins sharply reduces a number of possible crystal lattice rearrangement mechanisms. The stable twins

have perfect twin boundaries free of partial dislocations in spite of the shuffling involved in the $\delta \rightarrow \alpha$ transformation and thus have smaller interfacial energy.

The analysis of twin stability and the IPS condition within physically reasonable range of parameter $\delta \leq 1.025$ predicts the $(205)_\alpha$ or $(01\bar{1})_\delta$ stable transformation twins formed by twin-related variants 1 and 4.

The IPS solutions turn out to be highly sensitive to the value of δ. Since the parameter δ varies for plutonium alloys with different composition, transformation temperature, and depends on other factors, all IPS solutions within the range, $1 < \delta \leq 1.025$, are obtained for the cases where a deviation from the orientation relations $[\bar{1}10]_\delta \parallel [100]_\alpha$ and $(111)_\delta \parallel (020)_\alpha$ is less than 5^o. The results are summarized in Figs. 5-7. They provide sufficient information to determine the MT mechanism if accurate experimental measurements of lattice parameters, habit plane orientation, and the domain volume fraction in martensite plate are available.

Two simplest shuffling modes are singled out as possible MT mechanisms: the single elementary shuffling mode ("A") that has been studied in [10] and the double elementary shuffling mode ("D"). The single elementary shuffling is produced by the $1/6[\bar{2}11]_\delta$ partial lattice translation. The double elementary shuffling is produced by two alternating partial lattice translations, $1/6[1\bar{2}1]_\delta$ and $1/6[11\bar{2}]_\delta$. Both shuffling modes produce the $(205)_\alpha$ stable twin, the $[100]_\alpha \parallel [\bar{1}10]_\delta$ and $(010)_\alpha \parallel (111)_\delta$ orientation relations, and the invariant habit planes close to $\{123\}_\delta$. However, the double elementary shuffling produces smaller Bain distortion, smaller IPS shape strain, and invariant habit plane closer to the $\{123\}_\delta$ than the single shuffling mode does, so it is preferred.

Acknowledgements: This work was performed under the auspices of the U.S. Department of Energy by University of California, Lawrence Livermore National Laboratory under Contract W-7405-Eng-48. YMJ, YUW and AGK also acknowledge the support from National Science Foundation under grants DMR-0242619.

References

1. A.M. Boring and J.L. Smith: Los Alamos Science, 2000, vol. 26, pp. 91-127.
2. G.B. Olson and P.H. Adler: Scripta Metal., 1984, vol. 18, pp. 401-6.
3. Y.M. Jin, A. Artemev and A.G. Khachaturyan: Acta Mater., 2001, vol. 49, pp. 2309-20.
4. A.G. Crocker: J. Nucl. Mater., 1971, vol. 41, pp. 167-77.
5. A. Goldberg, R.L. Rose and J. Shyne: J. Nucl. Mater., 1975, vol. 55, pp. 33-52.
6. M.A. Choudry and A.G. Crocker: J. Nucl. Mater., 1985, vol. 127, pp. 119-24.
7. P.H. Adler, G.B. Olson and D.S. Margolies: Acta Metal., 1986, vol. 34, pp. 2053-64.

8. T.G. Zocco, R.I. Sheldon, M.F. Stevens and H.F. Rizzo: J. Nucl. Mater., 1989, vol. 165, pp. 238-46.
9. C.E. Olsen: J. Nucl. Mater., 1989, vol. 168, pp. 326-7.
10. T.G. Zocco, M.F. Stevens, P.H. Adler, R.I. Sheldon and G.B. Olson: Acta Metal., 1990, vol. 38, pp. 2275-82.
11. S.S. Hecker, E.G. Zukas, J.R. Morgan and I. Pereyra: Proc. Int. Conf. Solid-Solid Phase Trans., Carnegie-Mellon Univ., 1981 (edited by H.I. Aaronson), Am. Inst. Min. Engrs, New York, pp 1339-43.
12. M.A. Wall: Lawrence Livermore National Laboratory, unpublished research, 2003.
13. C.R. Krenn, M.A. Wall and A. J. Schwartz: MRS Proceedings, 2004, vol. 802, DD1.3, pp. 9-14.
14. T.G. Zocco and A.J. Schwartz: JOM, 2003, vol. 55, No. 9, pp. 24-7.
15. S.S. Hecker: JOM, 2003, vol. 55, No. 9, pp. 13-8.
16. A.C. Lawson, J.A. Roberts, B. Martinez, J.W. Richardson, H. Ledbetter and A. Migliori: JOM, 2003, vol. 55, No. 9, pp. 31-3.
17. A.C. Lawson, J.A. Roberts, B. Martinez and J.W. Richardson: Phil. Mag. B, 2002, vol. 82, pp. 1837-45.
18. S.S. Hecker, D.R. Harbur and T.G. Zocco: Prog. Mater. Sci., 2004, vol. 49, pp. 429-85.
19. A.G. Khachaturyan: Theory of Structural Transformations in Solids, John Wiley & Sons, New York, 1983.
20. Y.M. Jin and G.J. Weng: Acta Mater., 2002, vol. 50, pp. 2967-87.
21. M.S. Wechsler, D.S. Lieberman and T.A. Read: J. Metals, 1953, vol. 197, pp. 1503-15.
22. J.S. Bowles and J.K. MacKenzie: Acta Metal., 1954, vol. 2, pp 129-37, pp. 138-47, pp. 224-34.
23. A.G. Khachaturyan and G.A. Shatalov: Sov. Phys. JEPT, 1969, vol. 29, pp. 557-61.
24. A.L. Roitburd: Sov. Phys. Solid State, 1969, vol. 10, pp. 2870-6.
25. B. Sadigh and W.G. Wolfer: Lawrence Livermore National Laboratory, unpublished research, 2002.

Appendix

Table A1. Calculated lattice transformation matrices for δ→α phase transformation.

	Deformation matrix in coordinates $x_1 // [\bar{1}10]_\delta$, $x_2 // [111]_\delta$, $x_3 // [11\bar{2}]_\delta$			Deformation matrix in δ cubic coordinates			Eigenvalue
	.94764	.27675	.07585	.75920	-.18845	-.12255	.76213
A	-.00000	.90555	-.00000	.08131	1.02895	.01583	.98001
	-.00000	-.16745	.94722	.06504	.06504	1.01227	1.08830
	.94764	-.30356	.07585	.99611	.04846	.11436	.78071
B	.00000	.90555	-.00000	-.15560	.79204	-.22108	.91530
	.00000	-.16745	.94722	.06504	.06504	1.01227	1.13752
	.94764	.02682	.07585	.97963	.03199	.09789	.77093
C	.00000	.90555	-.00000	.09768	1.04532	.03220	.94279
	.00000	.33489	.94722	-.17176	-.17176	.77546	1.11836
	.94764	-.13837	.07585	.98787	.04023	.10612	.83190
D	-.00000	.90555	-.00000	-.02896	.91868	-.09444	.97330
	-.00000	.08372	.94722	-.05336	-.05336	.89387	1.00390
	.94764	.15178	.07585	.86942	-.07823	-.01233	.85110
E	.00000	.90555	-.00000	.08949	1.03714	.02402	.91499
	.00000	.08372	.94722	-.05336	-.05336	.89387	1.04380
	.94764	-.01341	.07585	.87765	-.06999	-.00409	.84036
F	0.00000	.90555	-.00000	-.03715	.91050	-.10262	.93843
	0.00000	-.16745	.94722	.06504	.06504	1.01227	1.03073
	.94764	-.00000	.07585	.91165	-.03600	.02990	.90555
O	0.00000	.90555	-.00000	.00779	.95544	-.05768	.91027
	0.00000	.00000	.94722	-.01389	-.01389	.93333	.98612

Table A2. Definition of 24 variants of the α phase.

variant	$[100]_\alpha$	$[010]_\alpha$	variant	$[100]_\alpha$	$[100]_\alpha$
1	$[\,-1\ \ 1\ \ 0\,]_\delta$	$[\ \ 1\ \ 1\ \ 1\,]_\delta$	13	$[\ \ 1\ \ 1\ \ 0\,]_\delta$	$[\,-1\ \ 1\,-1\,]_\delta$
2	$[\,-1\ \ 1\ \ 0\,]_\delta$	$[\,-1\,-1\,-1\,]_\delta$	14	$[\ \ 1\ \ 1\ \ 0\,]_\delta$	$[\ \ 1\,-1\ \ 1\,]_\delta$
3	$[\ \ 1\ \ 0\,-1\,]_\delta$	$[\ \ 1\ \ 1\ \ 1\,]_\delta$	15	$[\,-1\ \ 0\ \ 1\,]_\delta$	$[\,-1\ \ 1\,-1\,]_\delta$
4	$[\ \ 1\ \ 0\,-1\,]_\delta$	$[\,-1\,-1\,-1\,]_\delta$	16	$[\,-1\ \ 0\ \ 1\,]_\delta$	$[\ \ 1\,-1\ \ 1\,]_\delta$
5	$[\ \ 0\,-1\ \ 1\,]_\delta$	$[\ \ 1\ \ 1\ \ 1\,]_\delta$	17	$[\ \ 0\,-1\,-1\,]_\delta$	$[\,-1\ \ 1\,-1\,]_\delta$
6	$[\ \ 0\,-1\ \ 1\,]_\delta$	$[\,-1\,-1\,-1\,]_\delta$	18	$[\ \ 0\,-1\,-1\,]_\delta$	$[\ \ 1\,-1\ \ 1\,]_\delta$
7	$[\ \ 1\,-1\ \ 0\,]_\delta$	$[\,-1\,-1\ \ 1\,]_\delta$	19	$[\,-1\,-1\ \ 0\,]_\delta$	$[\ \ 1\,-1\,-1\,]_\delta$
8	$[\ \ 1\,-1\ \ 0\,]_\delta$	$[\ \ 1\ \ 1\,-1\,]_\delta$	20	$[\,-1\,-1\ \ 0\,]_\delta$	$[\,-1\ \ 1\ \ 1\,]_\delta$
9	$[\,-1\ \ 0\,-1\,]_\delta$	$[\,-1\,-1\ \ 1\,]_\delta$	21	$[\ \ 1\ \ 0\ \ 1\,]_\delta$	$[\ \ 1\,-1\,-1\,]_\delta$
10	$[\,-1\ \ 0\,-1\,]_\delta$	$[\ \ 1\ \ 1\,-1\,]_\delta$	22	$[\ \ 1\ \ 0\ \ 1\,]_\delta$	$[\,-1\ \ 1\ \ 1\,]_\delta$
11	$[\ \ 0\ \ 1\ \ 1\,]_\delta$	$[\,-1\,-1\ \ 1\,]_\delta$	23	$[\ \ 0\ \ 1\,-1\,]_\delta$	$[\ \ 1\,-1\,-1\,]_\delta$
12	$[\ \ 0\ \ 1\ \ 1\,]_\delta$	$[\ \ 1\ \ 1\,-1\,]_\delta$	24	$[\ \ 0\ \ 1\,-1\,]_\delta$	$[\,-1\ \ 1\ \ 1\,]_\delta$

Table A3. Invariant Plane Strain generated by the twin pairs of simple shuffling modes.

Twin pair information: A shuffling, variants 1 and 7 with shear S= .20495	
Twin element:	
α coordinate: (K_1)$_\alpha$ [η_1]$_\alpha$	δ coordinate: (K_1)$_\delta$ [η_1]$_\delta$
(K_2)$_\alpha$ [η_2]$_\alpha$	(K_2)$_\delta$ [η_2]$_\delta$
(.00000 .25000 -1.00000)$_\alpha$ [1.00000 -.16843 -.04211]$_\alpha$	(.00000 -.00000 1.00000)$_\delta$ [.35143 -.93621 .00000]$_\delta$
(1.00000 -.01056 -.84742)$_\alpha$ [-.62500 1.00000 -.75000]$_\alpha$	(.23911 -.97099 .00000)$_\delta$ [-.00000 -.00000 1.00000]$_\delta$
Habit planes:	
Type I twin: ε=0.30387 ε_n=-0.18715 ε_τ=0.23939	
x:(1-x)= 0.771093:0.228907	x:(1-x)= 0.228907:0.771093
No. 1 (.81391 .52098 .25715)$_\delta$ [-.57992 .70165 .41400]$_\delta$	(.81391 .52098 -.25715)$_\delta$ [-.57992 .70165 -.41400]$_\delta$
No. 2 (-.91273 .34022 .22624)$_\delta$ [.40705 .80497 .43166]$_\delta$	(-.91273 .34022 -.22624)$_\delta$ [.40705 .80497 -.43166]$_\delta$
Type II twin: ε=0.30412 ε_n=-0.18715 ε_τ=0.23971	
x:(1-x)= 0.790654:0.209346	x:(1-x)= 0.209346:0.790654
No. 3 (.81565 .50342 .28511)$_\delta$ [-.57722 .67476 .45990]$_\delta$	(-.81565 -.50342 .28511) [.57722 -.67476 .45990]$_\delta$
No. 4 (-.91095 .32661 .25200)$_\delta$ [.41066 .77593 .47884]$_\delta$	(.91095 -.32661 .25200) [-.41066 -.77593 .47884]$_\delta$
Twin pair information: A shuffling, variants 1 and 13 with shear S= .23813	
(-1.00000 -.50000 -.50000)$_\alpha$ [.45159 .09682 -1.00000]$_\alpha$	(-.00000- 1.00000 -.00000) [-.67120 -.00000 .74128]$_\delta$
(.18818 -.00874 -1.00000)$_\alpha$ [-1.00000 -.72727 -.18182]$_\alpha$	(-.46440 -.00000 .88563) [-.00000 -1.00000 -.00000]$_\delta$
Habit planes:	
Type I twin: ε=0.29915 ε_n=-0.18715 ε_τ=0.23338	
x:(1-x)= 0.781989:0.218011	x:(1-x)= 0.218011:0.781989
No. 5 (.83343 .45277 .31684)$_\delta$ [-.55254 .69273 .46350]$_\delta$	(.83343 -.45277 .31684)$_\delta$ [-.55254 -.69273 .46350]$_\delta$
No. 6 (-.90577 .35551 .23063)$_\delta$ [.42365 .74732 .51189]$_\delta$	(-.90577 -.35551 .23063)$_\delta$ [.42365 -.74732 .51189]$_\delta$
Type II twin: ε=0.30145 ε_n=-0.18715 ε_τ=0.23632	
x:(1-x)= 0.770408:0.229592	x:(1-x)= 0.229592:0.770408
No. 7 (.83502 .47140 .28376)$_\delta$ [-.55012 .72472 .41491]$_\delta$	(.83502 -.47140 .28376)$_\delta$ [-.55012 -.72472 .41491]$_\delta$
No. 8 (-.90124 .37909 .20990)$_\delta$ [.43321 .77699 .45674]$_\delta$	(-.90124 -.37909 .20990)$_\delta$ [.43321 -.77699 .45674]$_\delta$
Twin pair information: B shuffling, variants 1 and 7 with shear S= .47271	
(.00000 .25000 -1.00000)$_\alpha$ [1.00000 -.16843 -.04211]$_\alpha$	(-.00000 .00000 1.00000)$_\delta$ [-.81677 .57697 -.00000]$_\delta$
(1.00000 -.01056 -.84742)$_\alpha$ [-.62500 1.00000 -.75000]$_\alpha$	(-.90000 .43589 - .00000)$_\delta$ [-.00000 .00000 1.00000]$_\delta$
Habit planes:	
Type I twin: ε=0.24319 ε_n=-0.18715 ε_τ=0.15530	
x:(1-x)= 0.569466:0.430534	x:(1-x)= 0.430534:0.569466
No. 9 (.42863 .85809 .28277)$_\delta$ [.59023 -.50291 .63144]$_\delta$	(-.42863 -.85809 .28277)$_\delta$ [-.59023 .50291 .63144]$_\delta$
No. 10 (.10901 -.96418 .24183)$_\delta$ [.72125 .24413 .64822]$_\delta$	(-.10901 .96418 .24183)$_\delta$ [-.72125 -.24413 .64822]$_\delta$
Twin pair information: B shuffling, variants 1 and 19 with shear S= .43578	
(.66667 -.33333 -1.00000)$_\alpha$ [-1.00000 .57591 -.85864]$_\alpha$	(-1.00000 .00000 -.00000)$_\delta$ [.00000 -.39160 .92013]$_\delta$
(-.15256 .07837 -1.00000)$_\alpha$ [1.00000 -.88889 -.22222]$_\alpha$	(.00000 -.31364 .94954)$_\delta$ [-1.00000 .00000 -.00000]$_\delta$
Habit planes:	
Type II twin: ε=0.25875 ε_n=-0.18715 ε_τ=0.17868	
x:(1-x)= 0.579523:0.420477	x:(1-x)= 0.420477:0.579523
No. 11 (-.21886 -.81545 -.53585)$_\delta$ [-.45260 .57136 -.68462]$_\delta$	(.21886 -.81545 -.53585)$_\delta$ [.45260 .57136 -.68462]$_\delta$
No. 12 (-.20043 .96491 -.16963)$_\delta$ [-.46106 -.24567 -.85268]$_\delta$	(.20043 .96491 -.16963)$_\delta$ [.46106 -.24567 -.85268]$_\delta$
Twin pair information: C shuffling, variants 1 and 13 with shear S= .38479	
(1.00000 .50000 .50000)$_\alpha$ [.53049 -.06098 -1.00000]$_\alpha$	(.00000 1.00000 .00000)$_\delta$ [-.72833 -.00000 .68523]$_\delta$
(.37268 .03415 -1.00000)$_\alpha$ [1.00000 .80000 .40000]$_\alpha$	(-.86065 -.00000 .50920)$_\delta$ [.00000 1.00000 .00000]$_\delta$
Habit planes:	
Type I twin: ε=0.26137 ε_n=-0.18715 ε_τ=0.18246	
x:(1-x)= 0.535087:0.464913	x:(1-x)= 0.464913:0.535087
No. 13 (-.13822 -.42942 - .89246)$_\delta$ [-.09068 -.89184 .44316]$_\delta$	(-.13822 .42942 -.89246)$_\delta$ [-.09068 .89184 .44316]$_\delta$
No. 14 (.01933 -.40747 .91301)$_\delta$ [-.16418 -.90208 -.39912]$_\delta$	(.01933 .40747 .91301)$_\delta$ [-.16418 .90208 -.39912]$_\delta$

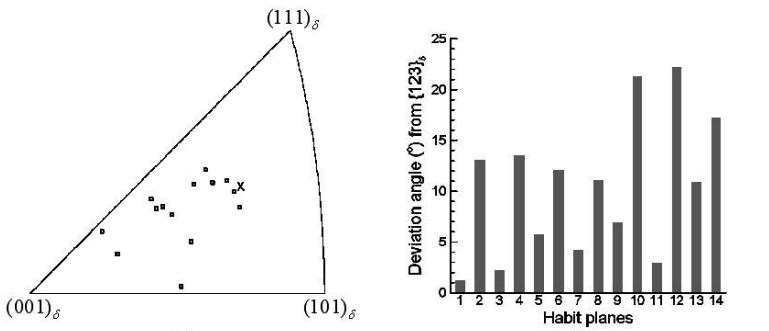

(a) (b)

Figure A1. (a) The stereographic projections of the normal directions of 14 possible habit planes (◦) obtained from our calculations and the experimentally observed habit plane normal direction: **X** $(123)_\delta$. (b) The deviation angles of the calculated habit plane normal directions from $(123)_\delta$. Some of the deviation angles are very small, for example, 1.192° (No. 1), 2.203° (No. 3), 2.883° (No. 11), 4.196° (No. 7), 5.773° (No. 5), and 6.933° (No. 5).